Asymptotic analysis of primitive model electrolytes and the electrical double layer

Phil Attard
Department of Physics, Faculty of Science, Australian National University, Canberra, Australian Capital Territory, 0200 Australia
(Received 24 May 1993)

The multicomponent primitive model electrolyte is analyzed using the Ornstein-Zernike equation and the asymptotic behavior of the direct correlation function. An approximation for the screening length is derived from the second-moment condition, $\kappa = \kappa_D/\sqrt{1-(\kappa_D d)^2/2+(\kappa_D d)^3/6}$, where κ_D^{-1} is the Debye length and d is the ion diameter. This is accurate up to $1M$ concentration for monovalent aqueous electrolytes and considerably extends the range of validity of the classical Debye-Hückel theory. The asymptotic behavior of the ionic pair correlation functions is formally analyzed, and exact expressions are given for the decay length and the effective charge on the ions in terms of the direct correlation function. Three different regimes are identified: monotonic exponential, for $\kappa_D d \lesssim \sqrt{2}$, and two types of damped oscillatory, electrostatic dominated at intermediate concentrations and core dominated at high concentrations, distinguished by whether or not the oscillations are in charge or in number density. The electrical double layer is also analyzed and it is shown that the asymptotic behavior of the density profiles and the interaction pressure is the same as for the bulk correlation functions. The hypernetted chain closure (with and without bridge functions) is used to obtain numerical results for binary symmetric aqueous electrolytes (monovalent with $d = 4$ and 5 Å, and divalent with $d = 4$ Å), and the three asymptotic regimes are explored.

PACS number(s): 61.20.Gy, 61.20.Qg, 82.45.+z, 82.70.Dd

INTRODUCTION

Electrolytes and the electrical double layer are widely studied. This is partly for practical reasons, since many liquids of technological and industrial importance contain ions or charged particles or surfaces, and also because electronic techniques are highly developed in modern laboratories. From the theoretical perspective, Coulomb interactions are the only part of the intermolecular potential that is known exactly, which makes for a well-defined model system for investigation, and the long-ranged tails create both challenges and opportunities for analytic study.

The simplest description of an electrolyte is the primitive model, in which the solvent is subsumed into a continuum dielectric constant, and the spherical ions bear a simple charge at their center and have some short-range repulsion, usually a hard core. The classical approach to electrolytes is the Debye-Hückel theory, which is a linearized mean-field approximation; the corresponding theory for the electrical double layer is called the Poisson-Boltzmann approximation. With the advent of computers, more exact numerical approaches have been developed, specifically simulations, which follow the motions of individual ions, and methods based upon the Ornstein-Zernike equation, which is solved for the radial distribution functions. These more sophisticated theories include the effects of ion size and ionic correlations, which are neglected in the classical approach, and which can sometimes be dramatic.

This paper exploits the long-range tail of the Coulomb potential to obtain a variety of exact and approximate results for the asymptotic behavior of the ionic correlation functions of the multicomponent, primitive model electrolyte. There are a number of reasons why this paper may prove useful theoretically. First, the analysis complements the numerical approaches. These usually have trouble with the asymptotic tails (e.g., beyond about half the simulation cell) and the formulas given here can be used to correct them since they are expressed in terms of short-ranged functions that should be accessible in the simulation. Also, the analysis may help to interpret certain results, which can be obscured in a numerical treatment of the problem. Second, certain quantities emerge naturally during the analysis (e.g., an effective charge for the ions) and the definitions given here may be used to quantify them using existing simulation schemes or integral equation approaches and show how the quantities found in a particular investigation may be applied more generally. Third, the computational problem can be simplified in the sense that the results allow some aspects of a difficult problem (such as the interaction between two double layers) to be cast in terms of a simpler one (in this example, the density profile of an isolated double layer). Fourth, the exact analysis also suggests some analytic approximations for the pair correlation functions and consequently for the thermodynamic properties of the electrolyte. The one explored in detail here should provide a useful basis for the discussion of numerical results, since it is as simple as the Debye-Hückel theory, but will be shown to be more accurate.

It is these approximate formulas that may be the most useful to experimentalists. For example, the Debye length is almost universally used in the characterization

of data, even though it is known that the actual screening length of the electrolyte can be rather different. Here a simple analytic result is given that expresses the actual screening length in terms of the Debye length and the size of the ions, and this is shown to be accurate in typical aqueous monovalent electrolytes up to $1M$. This important correction to the Debye length also improves the classical analytic results for properties such as the internal energy per ion, and the osmotic coefficient, and considerably extends their range of validity. The other finding of experimental interest is the transition from monotonic to oscillatory behavior of the ion correlation functions, and the two types of oscillations that occur. These should be testable by scattering experiments or by measurement of the electrical double layer force between charged surfaces. The reason that the latter data are relevant is because, as is shown here, it is the *bulk* pair correlation functions that determine the type and length of the decay of isolated and interacting electrical double layers.

The paper is divided into three sections. Section I introduces the formalism and derives in a simple fashion the well-known moment conditions. The Debye-Hückel approximation is also derived, and it is pointed out that this does not obey the second moment condition. An approximation for the pair correlation function is given, which has the same Yukawa form as the Debye-Hückel approximation, but which satisfies the first two moment conditions, thereby providing a formula for the actual screening length of the electrolyte in terms of the Debye length. This formula is used to provide an estimate of the monotonic-oscillatory transition. Section II consists of a formally exact analysis of the asymptotic behavior of the pair correlation functions based upon the Ornstein-Zernike equation. Monotonic asymptotic decay, oscillatory decay that is dominated by electrostatics, and core-dominated decay are treated in turn. The distinction between the last two is that in the electrostatic case the oscillations are in charge density, whereas in the latter the asymptotes are determined by the short-range part of the potential, and if these are the same for all ions then all the correlation functions become asymptotically identical. The asymptotic behavior of spherical solutes and planar electrical double layers is also analyzed. Sections I and II are for a general multicomponent electrolyte, whereas Sec. III gives results specific to a symmetric binary mixture. In particular, it contains an explicit analysis of the asymptotics, a description of the hypernetted chain algorithm, and numerical results. The latter includes tests of the analytic approximations and results for the concentration dependence of the asymptotes of three aqueous electrolytes (monovalents with core size 4 and 5 Å, and a divalent with $d = 4$ Å). A short summary concludes the paper.

Historically, the theory of electrolytes and ionic correlation functions began with the classic work of Debye and Hückel [1]. Stillinger and Lovett [2,3] obtained the second moment condition that bears their names, and a fourth moment result has also been given [4,5]. There have been a number of studies of the departure of the screening length from the Debye length [4–13]. The results of the formal asymptotic analysis of the present work are equivalent to those of Kjellander and Mitchell [13], although the derivation is somewhat different. Interest in the transition from monotonic to oscillatory decay of pair correlation functions can be traced to the work of Fisher and Widom [14] (see the literature cited by Evans *et al.* [15]). Stillinger and Lovett established an upper bound on this transition for electrolytes [2], and others have discussed the occurrence of charge oscillations [8,10,16]. A hypernetted chain study of the asymptotic phase diagram of the primitive model electrolyte, similar to that given here, has been independently carried out by Ennis [17], who in addition has obtained values for the effective surface charge of the planar double layer. The work of Evans *et al.* [15] is of relevance to the present discussion of the electrical double layer, since there it is stressed that it is the behavior of the bulk correlation functions that determine the decay of the density profile in an inhomogeneous fluid, a point that has been made by others [13,18].

I. MOMENT CONDITIONS AND APPROXIMATIONS

A. Correlation matrices

For a multicomponent fluid, the Ornstein-Zernike equation is

$$h_{\alpha\gamma}(r) = c_{\alpha\gamma}(r) + \sum_{\lambda} \rho_\lambda \int h_{\alpha\lambda}(s) c_{\lambda\gamma}(|\mathbf{r}-\mathbf{s}|)\, d\mathbf{s}, \quad (1.1)$$

where h and c are the total and the direct correlation functions, ρ is the number density, and the Greek subscripts index the species. This can be written in matrix form

$$\underline{\underline{H}}(r) = \underline{\underline{C}}(r) + \int \underline{\underline{H}}(s)\underline{\underline{C}}(|\mathbf{r}-\mathbf{s}|)\, d\mathbf{s}, \quad (1.2)$$

where the symmetric matrices have components

$$\{\underline{\underline{H}}(r)\}_{\alpha\gamma} = \rho_\alpha^{1/2}\rho_\gamma^{1/2} h_{\alpha\gamma}(r) \quad (1.3)$$

and

$$\{\underline{\underline{C}}(r)\}_{\alpha\gamma} = \rho_\alpha^{1/2}\rho_\gamma^{1/2} c_{\alpha\gamma}(r). \quad (1.4)$$

Consider a primitive model electrolyte, in which the long-range part of the pair potential is

$$u_{\alpha\gamma}^{\mathrm{Coul}}(r) = \frac{q_\alpha q_\gamma}{\epsilon r}, \quad (1.5)$$

where q_α is the charge of species α and $\epsilon = 4\pi\epsilon_0\epsilon_r$ is the total permittivity of the medium. In view of this, one defines the dyadic matrix

$$\underline{\underline{Q}} = \frac{4\pi\beta}{\epsilon}\underline{q}\,\underline{q}^T, \quad (1.6)$$

where $\beta = 1/k_BT$ is the inverse of the thermal energy

and where the column vectors have components

$$\{\underline{q}\}_\alpha = \rho_\alpha^{1/2} q_\alpha, \tag{1.7}$$

with T denoting the transpose.

The matrix $\underline{\underline{Q}}$ has a number of convenient properties. Its trace is related to the Debye length

$$\mathrm{Tr}\{\underline{\underline{Q}}\} = \frac{4\pi\beta}{\epsilon}\underline{q}^T\,\underline{q} = \frac{4\pi\beta}{\epsilon}\sum_\alpha \rho_\alpha q_\alpha^2 = \kappa_D^2, \tag{1.8}$$

and it is essentially idempotent,

$$\underline{\underline{Q}}^{n+1} = \kappa_D^{2n}\underline{\underline{Q}}. \tag{1.9}$$

Although $\underline{\underline{Q}}$ itself is singular, $\det\{\underline{\underline{Q}}\} = 0$, one can show that

$$(\underline{\underline{I}} + \alpha\underline{\underline{Q}})^{-1} = \underline{\underline{I}} - \frac{\alpha}{1+\alpha\kappa_D^2}\underline{\underline{Q}}. \tag{1.10}$$

In the electrolyte, the total correlation function is exponentially short ranged, but the direct correlation function goes like the negative of the pair potential at large separations. Accordingly, one defines the function

$$\underline{\underline{\chi}}(r) = \underline{\underline{C}}(r) + \frac{1}{4\pi r}\underline{\underline{Q}}, \tag{1.11}$$

which has a shorter range than the total correlation function $\chi_{\alpha\gamma}(r)/h_{\alpha\gamma}(r) \to 0\ ,\quad r \to \infty$. The three-dimensional Fourier transform is

$$\hat{\underline{\underline{\chi}}}(k) = \hat{\underline{\underline{C}}}(k) + \underline{\underline{Q}}k^{-2}. \tag{1.12}$$

The matrices $\underline{\underline{H}}$ and $\underline{\underline{C}}$ commute, because the former is the sum of products of the latter. However, it is important to note that neither commute with $\underline{\underline{\chi}}$ or $\underline{\underline{Q}}$, nor do these themselves commute.

The Fourier transform of the Ornstein-Zernike equation is

$$\begin{aligned}\hat{\underline{\underline{H}}}(k) &= \hat{\underline{\underline{C}}}(k) + \hat{\underline{\underline{H}}}(k)\hat{\underline{\underline{C}}}(k) \\ &= \hat{\underline{\underline{\chi}}}(k) - \underline{\underline{Q}}k^{-2} + \hat{\underline{\underline{H}}}(k)\hat{\underline{\underline{\chi}}}(k) - \hat{\underline{\underline{H}}}(k)\underline{\underline{Q}}k^{-2}.\end{aligned} \tag{1.13}$$

Because both the correlation functions are short ranged, they possess a small-k Taylor series expansion. One has

$$\hat{\underline{\underline{H}}}(k) \underset{k\to 0}{\sim} \underline{\underline{H}}^{(0)} + \underline{\underline{H}}^{(2)}k^2 + \underline{\underline{H}}^{(4)}k^4 + \cdots, \tag{1.14}$$

and similarly for $\hat{\underline{\underline{\chi}}}(k)$. This expression may be obtained by expanding the integrand of the Fourier transform, and the moments are defined as

$$\underline{\underline{H}}^{(2n)} = \frac{4\pi(-1)^n}{(2n+1)!}\int_0^\infty \underline{\underline{H}}(r) r^{2n+2}\,dr. \tag{1.15}$$

All moments exist for an exponentially short-ranged function. One now inserts the Taylor expansion into the Ornstein-Zernike equation and equates powers of k.

B. The zeroth moment condition (electroneutrality)

Equating the coefficients of k^{-2}, one obtains

$$0 = -\underline{\underline{Q}} - \underline{\underline{H}}^{(0)}\underline{\underline{Q}}. \tag{1.16}$$

Explicitly, this is the zeroth moment condition

$$q_\alpha = -\sum_\gamma \rho_\gamma q_\gamma \int h_{\alpha\gamma}(r)\,d\mathbf{r}, \tag{1.17}$$

which expresses the fact that each ion is surrounded by a cloud of ions bearing a net equal and opposite charge. In other words, the electrolyte is overall neutral. Note that in the case of the zeroth moment, the two matrices commute, $\underline{\underline{Q}}\,\underline{\underline{H}}^{(0)} = \underline{\underline{H}}^{(0)}\,\underline{\underline{Q}}$.

C. The second moment condition (Stillinger-Lovett)

The second moment condition arises from the equality of the coefficients of k^0 in the small-k Taylor expansion of the Ornstein-Zernike equation

$$\underline{\underline{H}}^{(0)} = \underline{\underline{\chi}}^{(0)} + \underline{\underline{H}}^{(0)}\underline{\underline{\chi}}^{(0)} - \underline{\underline{H}}^{(2)}\underline{\underline{Q}}. \tag{1.18}$$

Premultiplying by $\underline{\underline{Q}}$, one obtains

$$\underline{\underline{Q}}\,\underline{\underline{H}}^{(0)} = \underline{\underline{Q}}\,\underline{\underline{\chi}}^{(0)} + \underline{\underline{Q}}\,\underline{\underline{H}}^{(0)}\underline{\underline{\chi}}^{(0)} - \underline{\underline{Q}}\,\underline{\underline{H}}^{(2)}\underline{\underline{Q}} \tag{1.19}$$

or, using Eq. (1.16),

$$-\underline{\underline{Q}} = -\underline{\underline{Q}}\,\underline{\underline{H}}^{(2)}\underline{\underline{Q}}. \tag{1.20}$$

Explicitly, this is

$$1 = \frac{-4\pi\beta}{6\epsilon}\sum_{\gamma,\lambda} q_\gamma q_\lambda \rho_\gamma \rho_\lambda \int h_{\gamma\lambda}(r) r^2\,d\mathbf{r}. \tag{1.21}$$

Both the zeroth and second moments are determined by the long-range tail of the Coulomb potential and are independent of any short-range interactions between the ions [2,3].

D. The fourth moment condition

Equating the coefficients of k^2, one obtains

$$\underline{\underline{H}}^{(2)} = \underline{\underline{\chi}}^{(2)} + \underline{\underline{H}}^{(2)}\underline{\underline{\chi}}^{(0)} + \underline{\underline{H}}^{(0)}\underline{\underline{\chi}}^{(2)} - \underline{\underline{H}}^{(4)}\underline{\underline{Q}}. \tag{1.22}$$

The second moment of the shortened direct correlation function can be eliminated by premultiplying by $\underline{\underline{Q}}$ and using Eq. (1.16),

$$\underline{\underline{Q}}\,\underline{\underline{H}}^{(2)} = \underline{\underline{Q}}\,\underline{\underline{H}}^{(2)}\underline{\underline{\chi}}^{(0)} - \underline{\underline{Q}}\,\underline{\underline{H}}^{(4)}\underline{\underline{Q}}. \tag{1.23}$$

Finally, the second moment equation [cf. Eq. (1.18)] can be used to relate the fourth moment of the total correla-

tion function to the two zeroth moments,

$$\underline{\underline{Q}}\,\underline{\underline{H}}^{(4)}\underline{\underline{Q}} = (\underline{\underline{H}}^{(0)} - \underline{\underline{\chi}}^{(0)} - \underline{\underline{\chi}}^{(0)}\underline{\underline{H}}^{(0)})(\underline{\underline{I}} - \underline{\underline{\chi}}^{(0)}). \quad (1.24)$$

In contrast to the other two moment conditions, this fourth moment will depend upon the short-range behavior of the ions. Earlier work has related the coefficient of k^2 in the expansion of the partial ionic structure factors to the isothermal compressibility of the electrolyte [4,5].

E. Debye-Hückel theory

The linearized Debye-Hückel theory may be derived by neglecting the short-ranged part of the direct correlation function,

$$\hat{\underline{\underline{\chi}}}(k) = 0. \quad (1.25)$$

The Ornstein-Zernike equation, (1.13), becomes

$$\begin{aligned}\hat{\underline{\underline{H}}}(k) &= -\left(\underline{\underline{I}} + \underline{\underline{Q}}k^{-2}\right)^{-1}\underline{\underline{Q}}k^{-2} \\ &= -\left(\underline{\underline{I}} - \frac{1}{k^2+\kappa_D^2}\underline{\underline{Q}}\right)\underline{\underline{Q}}k^{-2} \\ &= \frac{-1}{k^2+\kappa_D^2}\underline{\underline{Q}}, \end{aligned} \quad (1.26)$$

where Eqs. (1.9) and (1.10) have been used. This has inverse transform

$$\underline{\underline{H}}(r) = \frac{-e^{-\kappa_D r}}{4\pi r}\underline{\underline{Q}}, \quad (1.27)$$

or in component form

$$h_{\alpha\gamma}(r) = \frac{-\beta q_\alpha q_\gamma}{\epsilon r}e^{-\kappa_D r}. \quad (1.28)$$

Hence the Debye-Hückel theory predicts that the ion correlation functions are exponentially decaying, with the decay length being the Debye length, and with the amplitude proportional to the product of the charges on the ions.

The Debye-Hückel approximation only satisfies the electroneutrality condition if this exponential form holds for all of r, not just asymptotically. For ions all with a hard core of diameter d, $h_{\alpha\gamma}(r) = -1$, $r < d$, which means that the electroneutrality condition is no longer satsified by Eq. (1.28) applied beyond the core. If one demands this functional form but scales the prefactor so as to satisfy electroneutrality, then the modified linearized Debye-Hückel approximation is

$$h_{\alpha\gamma}(r) = \begin{cases} -1, & r < d \\ \dfrac{-\beta q_\alpha q_\gamma e^{\kappa_D d}}{\epsilon[1+\kappa_D d]}\dfrac{e^{-\kappa_D r}}{r}, & r > d. \end{cases} \quad (1.29)$$

One problem that remains with this linearized theory is that it allows the co-ion radial distribution function to become negative. For this reason, this functional form is often applied instead to the potential of mean force, which when exponentiated gives the radial distribution function. This nonlinear version has the same asymptote, but remains physical at small separations for high electrolyte couplings. The other problem with this result is that it does not obey the second moment condition. Now an elementary approximation with the same functional form is explored, but which obeys both moment conditions by determining the actual decay length of the electrolyte in terms of the Debye length and the ionic diameter.

F. Self-consistent screening length

In this paper one concern is with the transition from monotonic exponentially decaying pair correlations to oscillatory behavior, and the zeroth and second moment conditions have been used to set a limit for this transition [2]. In view of the explicit representations of the moment conditions, Eqs. (1.17) and (1.21), one defines the countercharge density

$$\eta_\alpha(r) = \sum_\gamma q_\gamma \rho_\gamma h_{\alpha\gamma}(r) \quad (1.30)$$

and assumes that $-q_\alpha\eta_\alpha(r) \geq 0$. For ions all with the same hard-core diameter d, it follows from Eq. (1.21) that

$$\begin{aligned} 1 &= \frac{4\pi\beta}{6\epsilon}\sum_\alpha \rho_\alpha 4\pi\int_d^\infty -q_\alpha\eta_\alpha(r)r^4\,dr \\ &\geq d^2\frac{4\pi\beta}{6\epsilon}\sum_\alpha \rho_\alpha 4\pi\int_d^\infty -q_\alpha\eta_\alpha(r)r^2\,dr \\ &= d^2\frac{4\pi\beta}{6\epsilon}\sum_\alpha \rho_\alpha q_\alpha^2 \\ &= \kappa_D^2 d^2/6, \end{aligned} \quad (1.31)$$

where the inequality follows from the non-negativity assumption and the third line follows from Eq. (1.17). Since oscillations violate the assumption, this provides an upper limit for the concentration (i.e., inverse Debye length) for which one can have monotonic ion profiles, namely [2]

$$\kappa_D d \leq \sqrt{6}. \quad (1.32)$$

By making a stronger assumption on the countercharge profile, namely that it has the Debye-Hückel form, one obtains an approximation that obeys both moment conditions and also a tighter bound for the onset of oscillations. One assumes that the countercharge profile is purely exponential beyond the hard core,

$$\eta_\alpha(r) = \eta_\alpha\frac{e^{-\kappa r}}{r}, \quad (1.33)$$

where again $-q_\alpha\eta_\alpha > 0$, and an explicit approximation is now obtained for the screening length κ^{-1} in terms of the Debye length. The second moment condition becomes

$$1 = \frac{4\pi\beta}{6\epsilon}\sum_\alpha -q_\alpha\rho_\alpha 4\pi\int_d^\infty \eta_\alpha e^{-\kappa r}r^3\,dr$$
$$= \frac{4\pi\beta}{6\epsilon}\sum_\alpha -q_\alpha\rho_\alpha 4\pi\eta_\alpha\kappa^{-4}$$
$$\times[6+6\kappa d+3(\kappa d)^2+(\kappa d)^3]e^{-\kappa d},$$
$$= \frac{\kappa_D^2}{\kappa^2}\frac{1+\kappa d+(\kappa d)^2/2+(\kappa d)^3/6}{1+\kappa d}, \quad (1.34)$$

where η_α has been eliminated using the electroneutrality condition

$$-q_\alpha = 4\pi\int_d^\infty \eta_\alpha e^{-\kappa r}r\,dr$$
$$= 4\pi\eta_\alpha\kappa^{-2}[1+\kappa d]e^{-\kappa d}. \quad (1.35)$$

The assumption of purely exponential profiles is only expected to be valid for small κd. Expanding Eq. (1.34) to second order, one has

$$\kappa^2 = \kappa_D^2[1+(\kappa d)^2/2+\mathcal{O}(\kappa d)^3], \quad (1.36)$$

with solution

$$\kappa = \frac{\kappa_D}{\sqrt{1-(\kappa_D d)^2/2}}. \quad (1.37)$$

This equation gives the actual screening length of the electrolyte in terms of the hard-core diameter and the Debye length; it equals the latter in the limit $\kappa_D d \to 0$. Although only the leading correction to the Debye length is strictly valid, the above may be viewed as a linear Padé approximant to the actual screening length of the electrolyte. The divergence of the denominator may be interpreted as signifying the breakdown of the monotonicity assumption and, hence, oscillations commence when

$$\kappa_D d \geq \sqrt{2}. \quad (1.38)$$

The next order solution to the cubic equation for the screening length that has the same functional form as Eq. (1.37) is

$$\kappa = \frac{\kappa_D}{\sqrt{1-(\kappa_D d)^2/2+(\kappa_D d)^3/6}}. \quad (1.39)$$

The amplitude of the countercharge profile follows from Eq. (1.35)

$$\eta_\alpha = \frac{-q_\alpha\kappa^2 e^{\kappa d}}{4\pi[1+\kappa d]}. \quad (1.40)$$

This and the definition Eq. (1.30) imply that $\underline{q}$ is an eigenvector of $\underline{\underline{H}}(r)$, and if one assumes that the latter is dyadic, then

$$h_{\alpha\gamma}(r) = \frac{-\beta q_\alpha q_\gamma}{\epsilon[1+\kappa d]}\frac{\kappa^2 e^{\kappa d}}{\kappa_D^2}\frac{e^{-\kappa r}}{r}, \quad r \geq d. \quad (1.41)$$

This result would be identical to the modified Debye-Hückel result, Eq. (1.29), if the screening length were the Debye length $\kappa = \kappa_D$. To the extent that Eq. (1.39) is valid, this result represents an improvement on the Debye-Hückel approximation.

As mentioned above, a problem with this linearized type of approximation is that it allows negative values for the co-ion radial distribution function at higher electrolyte couplings. Experience shows that a better approximation is to assume that it is the potential of mean force that has the exponential form

$$w_{\alpha\gamma}(r) = \frac{q_\alpha q_\gamma}{\epsilon\nu}\frac{e^{-\kappa r}}{r}, r > d. \quad (1.42)$$

One seeks values for κ and ν so that the correlation functions $h_{\alpha\gamma}(r) = -1 + \exp -\beta w_{\alpha\gamma}(r)$ satisfy the two moment conditions. It proved straightforward to use Newton's method to solve Eqs. (1.17), (1.21), and (1.42) numerically. The nonlinear approximation has the same asymptotic form as the analytic versions, with slightly different values for the parameters, while remaining physically realistic at small separations. One may anticipate that the approximations that obey the exact moment conditions will be more accurate than those that do not, as will indeed be demonstrated below.

There have been a number of earlier results for the screening length of Coulomb fluids (electrolytes, one-component plasmas, and molten salts). Hydrodynamic arguments and the fourth moment have been used to obtain a formal result in terms of the isothermal compressibility [4,5]. Stell and Lebowitz [6] obtained an expression in terms of integrals of the total correlation function of a reference fluid, but their correction vanished if the short-range interactions between the ions were identical. A similar deficiency occurred in the work of Mitchell and Ninham [7], who expanded the short-range part of the direct correlation function in the Ornstein-Zernike equation. Parinello and Tosi [8] gave an analytic result using the mean-spherical approximation. Outhwaite [10] has discussed several transcendental formulas for the screening length based upon the linearized modified Poisson-Boltzmann theory, including one analyzed by Stillinger and Lovett [9]. Blum [11] and Blum and Høye [12] found that the properties of the unrestricted primitive model electrolyte in the mean spherical approximation could be expressed in terms of a single length parameter, which was the screening length in that approximation, and which could be expanded in terms of the Debye length and the diameters of the ions. Their result for the symmetric binary electrolyte is $\kappa = \kappa_D[-1+\sqrt{(1+2\kappa_D d)}]$, which may be compared with Eq. (1.39) and to the numerical results below. Finally, it is worth mentioning a footnote by Stillinger and Lovett [3], who point out that the Debye-Hückel theory only satisfies the second moment condition for ions of zero size, unless one allows for an effective screening length rather than the Debye length, which is precisely the content of the results in this section.

II. EXACT ASYMPTOTIC ANALYSES

A. Electrostatic domination

1. Monotonic asymptotic decay

The Ornstein-Zernike equation, (1.13), may be solved for the total correlation function

$$\hat{\underline{\underline{H}}}(k) = [\underline{\underline{I}} - \hat{\underline{\underline{\chi}}}(k) + \underline{\underline{Q}}k^{-2}]^{-1}[\hat{\underline{\underline{\chi}}}(k) - \underline{\underline{Q}}k^{-2}] \tag{2.1a}$$

$$= \left(\underline{\underline{I}} + [\underline{\underline{I}} - \hat{\underline{\underline{\chi}}}(k)]^{-1}\underline{q}\,\underline{q}^T\frac{4\pi\beta}{\epsilon k^2}\right)^{-1} \times [\underline{\underline{I}} - \hat{\underline{\underline{\chi}}}(k)]^{-1}\left(\hat{\underline{\underline{\chi}}}(k) - \underline{q}\,\underline{q}^T\frac{4\pi\beta}{\epsilon k^2}\right) \tag{2.1b}$$

$$= \left(\underline{\underline{I}} + \tilde{\underline{q}}(k)\underline{q}^T\frac{4\pi\beta}{\epsilon k^2}\right)^{-1}[\underline{\underline{I}} - \hat{\underline{\underline{\chi}}}(k)]^{-1} \times \left(\hat{\underline{\underline{\chi}}}(k) - \underline{q}\,\underline{q}^T\frac{4\pi\beta}{\epsilon k^2}\right). \tag{2.1c}$$

Here an effective charge function has been defined,

$$\tilde{\underline{q}}(k) = [\underline{\underline{I}} - \hat{\underline{\underline{\chi}}}(k)]^{-1}\underline{q}, \tag{2.2a}$$

which may be equivalently written

$$\tilde{\underline{q}}(k) = \underline{q} + \hat{\underline{\underline{\chi}}}(k)\tilde{\underline{q}}(k). \tag{2.2b}$$

Now the first inverse is readily evaluated [cf. Eq. (1.10)]

$$\left(\underline{\underline{I}} + \tilde{\underline{q}}(k)\underline{q}^T\frac{4\pi\beta}{\epsilon k^2}\right)^{-1} = \underline{\underline{I}} - \frac{4\pi\beta/\epsilon}{k^2 + \Lambda(k)^2}\tilde{\underline{q}}(k)\underline{q}^T, \tag{2.3}$$

where a function has been defined that will become the screening length [cf. Eq. (1.8)],

$$\Lambda(k)^2 = \frac{4\pi\beta}{\epsilon}\tilde{\underline{q}}^T(k)\underline{q}. \tag{2.4}$$

Now if there exists κ such that $\Lambda(i\kappa) = \kappa$, then the total correlation function will have a pole at $k = i\kappa$, which determines its asymptotic behavior. Neglecting the regular part, one has

$$\hat{\underline{\underline{H}}}(k) \sim \frac{-4\pi\beta/\epsilon}{k^2 + \Lambda(k)^2}\tilde{\underline{q}}(k)\underline{q}^T[\underline{\underline{I}} - \hat{\underline{\underline{\chi}}}(k)]^{-1} \times \left(\hat{\underline{\underline{\chi}}}(k) - \underline{q}\,\underline{q}^T\frac{4\pi\beta}{\epsilon k^2}\right) \tag{2.5a}$$

$$= \frac{-4\pi\beta/\epsilon}{k^2 + \Lambda(k)^2}\tilde{\underline{q}}(k)\tilde{\underline{q}}^T(k)\left(\hat{\underline{\underline{\chi}}}(k) - \underline{q}\,\underline{q}^T\frac{4\pi\beta}{\epsilon k^2}\right) \tag{2.5b}$$

$$= \frac{-4\pi\beta/\epsilon}{k^2 + \Lambda(k)^2}\tilde{\underline{q}}(k) \times [\tilde{\underline{q}}^T(k)\hat{\underline{\underline{\chi}}}(k) - \underline{q}^T\Lambda(k)^2/k^2] \tag{2.5c}$$

$$\underset{k\to i\kappa}{\sim} \frac{-4\pi\beta/\epsilon}{k^2 + \Lambda(k)^2}\tilde{\underline{q}}\,\tilde{\underline{q}}^T. \tag{2.5d}$$

Here the second line follows from Eq. (2.2a) and the final line from Eq. (2.2b). Also, $\tilde{\underline{q}} \equiv \tilde{\underline{q}}(i\kappa)$. This is in similar form to the Debye-Hückel result, Eq. (1.26), and in order to cast it in identical form, that is, to exhibit the residue explicitly, one needs the Taylor expansion of the denominator about $k = i\kappa$,

$$k^2 + \Lambda(k)^2 \sim (k - i\kappa)\left(2i\kappa + \frac{4\pi\beta}{\epsilon}\underline{q}^T\tilde{\underline{q}}'\right) + \cdots \sim (k^2 + \kappa^2)\left(1 + \frac{4\pi\beta}{2i\kappa\epsilon}\underline{q}^T\tilde{\underline{q}}'\right) + \mathcal{O}(k - i\kappa)^2. \tag{2.6}$$

Here

$$\tilde{\underline{q}}' = \left.\frac{\partial\tilde{\underline{q}}(k)}{\partial k}\right|_{k=i\kappa} = \left.\frac{\partial\hat{\underline{\underline{\chi}}}(k)}{\partial k}\right|_{k=i\kappa}\tilde{\underline{q}} + \hat{\underline{\underline{\chi}}}(i\kappa)\left.\frac{\partial\tilde{\underline{q}}(k)}{\partial k}\right|_{k=i\kappa} = [\underline{\underline{I}} - \hat{\underline{\underline{\chi}}}(i\kappa)]^{-1}\left.\frac{\partial\hat{\underline{\underline{\chi}}}(k)}{\partial k}\right|_{k=i\kappa}\tilde{\underline{q}}\,. \tag{2.7}$$

Hence one defines

$$\nu \equiv 1 + \frac{4\pi\beta}{2i\kappa\epsilon}\underline{q}^T\tilde{\underline{q}}' = 1 + \frac{4\pi\beta}{2i\kappa\epsilon}\underline{q}^T[\underline{\underline{I}} - \hat{\underline{\underline{\chi}}}(i\kappa)]^{-1}\hat{\underline{\underline{\chi}}}'(i\kappa)\tilde{\underline{q}} = 1 + \frac{4\pi\beta}{2i\kappa\epsilon}\tilde{\underline{q}}^T\hat{\underline{\underline{\chi}}}'(i\kappa)\tilde{\underline{q}}\,. \tag{2.8}$$

One now has

$$\hat{\underline{\underline{H}}}(k) \underset{k\to i\kappa}{\sim} \frac{-4\pi\beta}{\epsilon\nu}\frac{\tilde{\underline{q}}\,\tilde{\underline{q}}^T}{k^2 + \kappa^2}, \tag{2.9}$$

with inverse

$$h_{\alpha\gamma}(r) \underset{r\to\infty}{\sim} \frac{-\beta\tilde{q}_\alpha\tilde{q}_\gamma}{\epsilon\nu}\frac{e^{-\kappa r}}{r}\,, \quad \mathrm{Im}\{\kappa\} = 0. \tag{2.10}$$

Recall that $\tilde{\underline{q}}$ is given by Eq. (2.2a), evaluated at $k = i\kappa$, and that $\kappa^2 = (4\pi\beta/\epsilon)\tilde{\underline{q}}^T\underline{q}$. Note that if $\underline{\underline{\chi}} = 0$, Eq. (2.2a) implies that $\tilde{\underline{q}} = \underline{q}$, Eq. (2.4) yields $\kappa = \kappa_D$, and Eq. (2.8) shows that $\nu = 1$. In other words, the exact asymptote, Eq. (2.10), reduces to the Debye-Hückel result, Eq. (1.28).

2. *Oscillatory asymptotic decay*

One must allow for the possibility that κ is complex, which corresponds to oscillatory solutions. In this case one must take twice the real part of this expression, as may be seen as follows. By definition $h_{\alpha\gamma}(r)$ is a real, even function of r, and hence its Fourier transform is even, $\hat{h}_{\alpha\gamma}(-k) = \hat{h}_{\alpha\gamma}(k)$, and any series expansion in k has real coefficients $\overline{\hat{h}_{\alpha\gamma}(k)} = \hat{h}_{\alpha\gamma}(\bar{k})$, where the overbar denotes the complex conjugate. In other words,

$$\hat{\underline{\underline{H}}}(-k) = \hat{\underline{\underline{H}}}(k) \tag{2.11a}$$

and

$$\overline{\hat{\underline{\underline{H}}}(k)} = \hat{\underline{\underline{H}}}(\bar{k})\,. \tag{2.11b}$$

These two results imply that there are four poles located

at $\pm i\kappa$ and $\pm i\overline{\kappa}$, and the singular part may be written

$$\begin{aligned}\underline{\underline{\hat{H}}}^{s}(k) &= \frac{\underline{\underline{A}}}{k-i\kappa}+\frac{\underline{\underline{A'}}}{k+i\kappa}+\frac{\underline{\underline{B}}}{k-i\overline{\kappa}}+\frac{\underline{\underline{B'}}}{k+i\overline{\kappa}} \\ &= \frac{\underline{\underline{A}}}{k^2+\kappa^2}+\frac{\underline{\underline{B}}}{k^2+\overline{\kappa}^2} \\ &= \frac{\underline{\underline{A}}}{k^2+\kappa^2}+\frac{\overline{\underline{\underline{A}}}}{k^2+\overline{\kappa}^2}, \end{aligned} \tag{2.12}$$

since Eq. (2.11a) implies that $A = -A'$ and $B = -B'$, and Eq. (2.11b) implies that $B = \overline{A}$. Hence when the conventional Fourier inverse is evaluated by closing the contour in the upper half-plane (choosing κ to be in the first quadrant), one picks up the residue at $k = +i\kappa$, which is $A/(2i\kappa)$, and also its complex conjugate from the residue from the pole at $k = -i\overline{\kappa}$, which is $\overline{A}/(2i\overline{\kappa})$. The sum of these two is twice the real part of either one, and one has

$$h_{\alpha\gamma}(r) \underset{r\to\infty}{\sim} 2\,\mathrm{Re}\left\{\frac{-\beta\tilde{q}_\alpha\tilde{q}_\gamma}{\epsilon\nu}\frac{e^{-\kappa r}}{r}\right\}, \quad \mathrm{Im}\{\kappa\}\neq 0. \tag{2.13}$$

The abrupt disappearance of the factor of 2 as the poles coalesce on the imaginary axis suggests nonanalyticity in the amplitude of the correlation functions at the transition from monotonic to oscillatory decay. In fact, the amplitude becomes infinite, as will now be shown.

Let the pole just move off the imaginary k axis, $\kappa = \kappa_r + i\kappa_i$, $\kappa_i \to 0$. Expanding Eq. (2.4) one obtains

$$\begin{aligned}\kappa_r + i\kappa_i &= \left(\frac{4\pi\beta}{\epsilon}\underline{q}^T\underline{\tilde{q}}(i\kappa_r-\kappa_i)\right)^{1/2} \\ &\sim \left(\frac{4\pi\beta}{\epsilon}\underline{q}^T\underline{\tilde{q}}(i\kappa_r)\right)^{1/2} \\ &\quad\times\left[1-\frac{\kappa_i}{2}\frac{\underline{q}^T\underline{\tilde{q}}'(i\kappa_r)}{\underline{q}^T\underline{\tilde{q}}(i\kappa_r)}+\mathcal{O}(\kappa_i^2)\right] \\ &= \kappa_r - \frac{\kappa_i}{2\kappa_r}\frac{4\pi\beta}{\epsilon}\underline{q}^T\underline{\tilde{q}}'. \end{aligned} \tag{2.14}$$

Equating the coefficients of κ_i, one obtains

$$\frac{4\pi\beta}{2\kappa_r\epsilon}\underline{q}^T\underline{\tilde{q}}' = -i, \quad \kappa_i\to 0, \tag{2.15}$$

or, from Eq. (2.8),

$$\nu\to 0, \quad \kappa_i\to 0. \tag{2.16}$$

That is, the amplitude of the total correlation function becomes infinite at the oscillatory to monotonic transition.

One has to be careful in interpreting this result. The vanishing of ν means that the next term in the Taylor expansion of the denominator makes an increasingly important contribution (and consequently to obtain the residue of the first order pole, which determines that the asymptotic behavior remains exponential, one also has to go to the linear term in the numerator). For infinitesimal but nonzero ν, the present formulas give the strict asymptote, but the regime of applicability moves to ever larger separations. So even though the amplitude diverges, so do the relevant separations, and consequently thermodynamic properties such as the internal energy remain finite at the monotonic-oscillatory transition.

B. Core domination

The analysis of Sec. II A is formally exact, and the Fourier transforms of the total correlation functions are guarranteed to have a pole at $k = i\kappa$, for κ satisfying Eqs. (2.2a) and (2.4). Nevertheless this pole does not necessarily determine the asymptotic behavior of the correlations because there could be another pole, $k = i\xi$, with $\mathrm{Re}\{\xi\} < \mathrm{Re}\{\kappa\}$, even assuming that κ represents the solution of the preceding equations with smallest real part. Such a qualitatively different pole would correspond to the matrix $\underline{\underline{I}} - \underline{\underline{\hat{\chi}}}(i\xi)$ being singular.

The implicit reason for splitting the matrix $\underline{\underline{I}} - \underline{\underline{\hat{C}}}(k)$ in the fashion of Sec. II A was the assumption that the matrix $\underline{\underline{Q}}$ was the most important in the asymptotic regime. This would be the case when electrostatics determined the asymptotic behavior, hence the title of the section. However, at high densities one might expect the short-range interactions to become important asymptotically, and this regime might be termed the "core-dominated asymptote" and is the subject of this section.

This regime will not be treated in full generality, but instead the following restriction will be observed. Denote the amplitude of the total correlation functions in the asymptotic regime by $a_{\alpha\gamma}$. Then because electrostatic effects are of shorter range, locally the asymptotic charge density about an ion must vanish, and one has

$$\sum_\alpha q_\alpha\rho_\alpha a_{\alpha\gamma} = 0. \tag{2.17}$$

It is emphasized that this is an exact result that holds in the core-dominated asymptotic regime. One way of satisfying this equation is if

$$a_{\alpha\gamma} = a, \text{ all species.} \tag{2.18}$$

What follows is predicated on this restriction. Two cases can be mentioned where this equation will obviously hold. First, there is the general binary electrolyte, in which case this is the only possible solution. Second, there is a multicomponent electrolyte with the short-range interactions between the ions being identical; since it is the latter that determine the asymptote, the total correlation functions between all the species must be asymptotically equal.

The condition Eq. (2.18) means that the short-range part of the direct correlation function goes like

$$\underline{\underline{\hat{\chi}}}(k) \sim \underline{u}\,\underline{u}^T x(k), \quad k\to i\xi, \tag{2.19}$$

where $\{\underline{u}\}_\alpha = \rho_\alpha^{1/2}$. (This follows from the Ornstein-Zernike equation solved for the direct correlation function near the pole.) Note that $\underline{u}^T\underline{q} = 0$, and hence near the pole

$$[\underline{\underline{I}} - \underline{\underline{\hat{C}}}(k)]^{-1} \sim [\underline{\underline{I}} - \underline{u}\,\underline{u}^T x(k) + \underline{q}\,\underline{q}^T 4\pi\beta/\epsilon k^2]^{-1}$$
$$= \underline{\underline{I}} + \frac{\underline{u}\,\underline{u}^T x(k)}{1 - \underline{u}^T \underline{u}\, x(k)} - \frac{\underline{q}\,\underline{q}^T 4\pi\beta/\epsilon k^2}{1 + \underline{q}^T \underline{q} 4\pi\beta/\epsilon k^2}. \quad (2.20)$$

Now it is the middle term which has the pole at $k = i\xi$, and neglecting the remaining regular parts one obtains

$$\underline{\underline{\hat{H}}}(k) \sim \frac{\underline{u}\,\underline{u}^T x(k)}{1 - \underline{u}^T \underline{u}\, x(k)} [\underline{u}\,\underline{u}^T x(k) - \underline{q}\,\underline{q}^T 4\pi\beta/\epsilon k^2]$$
$$= \frac{\underline{u}^T \underline{u}\, x(k)^2}{1 - \underline{u}^T \underline{u}\, x(k)} \underline{u}\,\underline{u}^T$$
$$\underset{k\to i\xi}{\sim} \frac{-2i\xi x(i\xi)}{\underline{u}^T \underline{u}\, x'(i\xi)(k^2 + \xi^2)} \underline{u}\,\underline{u}^T . \quad (2.21)$$

Here a Taylor expansion of the denominator has been used, together with the fact that ξ satisfies

$$\underline{u}^T \underline{u} x(i\xi) = n x(i\xi) = 1, \quad (2.22)$$

where the total number density is $n = \sum_\alpha \rho_\alpha = \underline{u}^T \underline{u}$. One concludes that

$$h_{\alpha\gamma}(r) \underset{r\to\infty}{\sim} 2\,\mathrm{Re}\left\{ \frac{-2i\xi}{4\pi n^2 x'(i\xi)} \frac{e^{-\xi r}}{r} \right\} . \quad (2.23)$$

Again the factor of 2 is dropped if ξ is real. In contrast to Sec. II A, this analysis holds for uncharged particles, subject to the restriction (2.18).

C. Solutes and the electrical double layer

1. Electrostatic domination

Consider adding charged solutes to the electrolyte. If these are at infinite dilution (species 0, $\rho_0 \to 0$), then they do not contribute to the solvent correlation functions since the Ornstein-Zernike convolution integral contains a prefactor of ρ_0 whenever the solute correlation functions appear in the integrand. That is, the properties of the bulk solvent are not affected by the addition of the infinitely dilute solute, and all of the preceding analysis for the ionic correlations remains. Hence the decay length κ^{-1}, the effective charge on the ions $\tilde{q}_\gamma$, $\gamma > 0$, and the scale factor ν stay the same.

Define a vector of solute-solvent total correlation functions

$$\{\underline{H}(r)\}_\gamma = \rho_\gamma^{1/2} h_{0\gamma}(r), \quad \gamma > 0, \quad (2.24)$$

and similarly for the direct correlation functions. The solute-ion Ornstein-Zernike equation becomes

$$\underline{H}(r) = \underline{C}(r) + \int \underline{\underline{C}}(s) \underline{H}(|\mathbf{r} - \mathbf{s}|)\, d\mathbf{s}, \quad (2.25)$$

with Fourier transform

$$\underline{\hat{H}}(k) = [\underline{\underline{I}} - \underline{\underline{\hat{C}}}(k)]^{-1} \underline{\hat{C}}(k). \quad (2.26)$$

Here the contribution of the bulk solvent direct correlation functions is explicitly seen to be the same as before, and hence the solute-solvent total correlation functions have a pole at $k = i\kappa$ that is identical (up to a prefactor) to the one in the bulk solvent. The remainder of the electrostatic analysis goes through unchanged. (The case of core-dominated bulk behavior will be treated below.) One ends up with

$$\underline{\hat{H}}(k) \underset{k\to i\kappa}{\sim} \frac{-4\pi\beta/\epsilon}{k^2 + \Lambda(k)^2} \tilde{q}_0 \underline{\tilde{q}}, \quad (2.27)$$

where the effective charge on the solute is related to the short-range part of the solute-solvent direct correlation functions by

$$\tilde{q}_0 = \underline{\tilde{q}}^T \underline{\hat{C}}(i\kappa)$$
$$= q_0 + \underline{\tilde{q}}^T \underline{\hat{\chi}}(i\kappa) . \quad (2.28)$$

The asymptotic result is

$$h_{0\gamma}(r) \underset{r\to\infty}{\sim} 2\,\mathrm{Re}\left\{ \frac{-\beta\tilde{q}_0\tilde{q}_\gamma}{\epsilon\nu} \frac{e^{-\kappa r}}{r} \right\} . \quad (2.29)$$

It is emphasized that κ, ν, and $\tilde{q}_\gamma$, $\gamma > 0$, are all properties of the bulk electrolyte and are unaffected by the solute. Only $\tilde{q}_0$ depends on the nature of the solute, via the short-ranged part of the solute-solvent direct correlation functions. The solute-solute total correlation function follows by setting $\gamma = 0$ in this result and depends on the square of the effective solute charge.

The result for the planar electrical double can be obtained from the large radius limit of the preceding analysis. Explicitly exhibiting the dependence of the solute quantities on the radius R, one begins with the effective solute charge, Eq. (2.28),

$$\tilde{q}_0(R) = \underline{\tilde{q}}^T \underline{\hat{C}}(i\kappa; R). \quad (2.30)$$

The three-dimensional radial Fourier transform is

$$\underline{\hat{C}}(i\kappa; R) = \frac{4\pi}{\kappa} \int_0^\infty \underline{C}(r; R) \sinh(\kappa r) r\, dr$$
$$\underset{R\to\infty}{\sim} \frac{2\pi}{\kappa} R e^{\kappa R} \int_{-R}^\infty [\underline{\chi}(R + z; R) - \beta\underline{q} V_0(R + z; R)] e^{\kappa z}\, dz . \quad (2.31)$$

Only the leading term in R is retained, and the lower limit may be extended to $-\infty$. The problematic electrostatic potential $V_0(R + z; R)$ (whose Fourier transform is a generalized function) will be analyzed below, but the short-range part of the wall-ion direct correlation function is readily treated. In the planar limit one has

$$\lim_{R\to\infty} \underline{\chi}(R + z; R) = \underline{\chi}(z), \quad (2.32)$$

where [19]

$$\underline{\chi}(z) = \underline{H}(z) + \beta\underline{q}\psi(z)$$
$$- 2\pi \int_{-\infty}^\infty dz' \int_{|z-z'|}^\infty ds\, s\, \underline{\underline{\chi}}(s) \underline{H}(z'). \quad (2.33)$$

Here $h_\alpha(z)$ is the wall-ion total correlation function [$h_\alpha(z) = -1$, $z < 0$] and $\psi(z)$ is the mean-electrostatic potential [$\psi(z) \to 0$, $z \to \infty$]. $\chi_\alpha(z)$ is exponentially short ranged on the fluid side of the interface, and [19]

$$\lim_{z\to-\infty} \left\{\underline{\chi}(z)\right\}_\alpha = \rho_\alpha^{1/2}\left[-1 + \beta q_\alpha \psi(0) + \sum_\gamma \rho_\gamma \hat{\chi}_{\alpha\gamma}(0)\right], \tag{2.34}$$

which mean that the one-dimensional Fourier transform is well defined in the upper half of the complex plane,

$$\overline{\underline{\chi}}(k) = \int_{-\infty}^{\infty} \underline{\chi}(z) e^{-ikz}\, dz, \quad \mathrm{Im}\{k\} > 0. \tag{2.35}$$

The solute electrostatic potential, which is constant inside the surface, is in the large radius limit

$$\begin{aligned} V_0(R+z;R) &= \frac{q_0(R)}{\epsilon(R+z)} \\ &\sim \text{const} - \frac{4\pi\sigma}{\epsilon} z, \quad z > 0, \end{aligned} \tag{2.36}$$

where the solute charge and the surface charge density are related by $q_0(R) = 4\pi R^2\sigma$. The requisite analytic part of the Fourier transform is most easily extracted by twice differentiating this

$$V_0''(z) = -\frac{4\pi\sigma}{\epsilon}\delta(z)\ , \tag{2.37}$$

and then using the fact that $f''(z) \Longleftrightarrow -k^2\overline{f}(k)$. Inserting the Dirac δ into Eq. (2.31) and dividing by κ^2, one obtains for the electrostatic contribution to $\underline{\hat{C}}(i\kappa;R)$,

$$\frac{8\pi^2\beta\sigma}{\epsilon\kappa^3}\underline{q} R e^{\kappa R}, \quad R \to \infty. \tag{2.38}$$

Consequently one has

$$\begin{aligned} \lim_{R\to\infty} \underline{\tilde{q}}^T \underline{\hat{C}}(i\kappa;R) &= \frac{2\pi}{\kappa} R e^{\kappa R}\left[\frac{4\pi\beta\sigma}{\epsilon\kappa^2}\underline{\tilde{q}}^T\underline{q} + \underline{\tilde{q}}^T\overline{\underline{\chi}}(i\kappa)\right] \\ &= \frac{4\pi}{\kappa} R e^{\kappa R}\tilde{\sigma}. \end{aligned} \tag{2.39}$$

Note that the factor of 2π has been replaced by 4π because a factor of $\frac{1}{2}$ has been included in the definition of the effective surface charge,

$$\tilde{\sigma} = \frac{1}{2}\left[\sigma + \underline{\tilde{q}}^T\overline{\underline{\chi}}(i\kappa)\right], \tag{2.40}$$

where the effective screening length, Eq. (2.4), has been used. This definition preserves the Poisson-Boltzmann form for the asymptote, with the actual surface charge density being replaced by the effective one. Also in the low concentration limit, where $\chi_{\alpha\gamma}(r) = 0$ (and hence $\kappa = \kappa_D$ and $\tilde{q} = q$) and the linear Poisson-Boltzmann profile holds, $\underline{H}(z) = -\beta q\psi(z)$, $z > 0$, Eq. (2.33) shows that $\underline{\chi}(z) = 0$, $z > 0$, and that it is constant and equal to the first two terms on the right hand side of Eq. (2.34) for $z < 0$. In this limit $\underline{q}^T\underline{\chi}(z) = \kappa_D^2\epsilon\psi(0)/4\pi = \kappa_D\sigma$, $z < 0$, and hence $\underline{q}^T\overline{\underline{\chi}}(i\kappa_D) = \sigma$. In other words, with this definition, $\tilde{\sigma} = \sigma$ in the Debye-Hückel limit. Inserting these results into the solute-ion total correlation function,

$$h_{0\gamma}(R+z;R) \sim 2\,\mathrm{Re}\left\{\frac{-\beta\tilde{q}_\gamma\underline{\tilde{q}}^T\overline{\underline{C}}(i\kappa;R)}{\epsilon\nu}\frac{e^{-\kappa(R+z)}}{R+z}\right\} \tag{2.41}$$

one obtains in the planar limit

$$h_\gamma(z) \underset{z\to\infty}{\sim} 2\,\mathrm{Re}\left\{\frac{-4\pi\beta\tilde{q}_\gamma\tilde{\sigma}}{\epsilon\nu\kappa}e^{-\kappa z}\right\}\ . \tag{2.42}$$

The limiting procedure is $R \to \infty$, $z \to \infty$, $z/R \to 0$. Since it is the bulk correlation functions that determine the pole, there are two in the upper half k plane located at $i\kappa$ and $i\overline{\kappa}$. The residues are still the complex conjugate of each other, since $\underline{\chi}(r)$ is real. As before, one therefore takes twice the real part if $\mathrm{Im}\{\kappa\} \neq 0$, and drops the factor of 2 if κ is real. Note that the Yukawa form of the spherical case has become a pure exponential decay in planar geometry, a consequence of the fact that the three-dimensional Fourier transform of the short-ranged direct correlation function has been replaced by a one-dimensional one. It is probably worth mentioning that this result can also be obtained directly from the wall-ion Ornstein-Zernike equation (analysis not shown).

For the case of two interacting charged walls, one proceeds from the wall-wall Ornstein-Zernike equation. The interaction free energy per unit area is [19,20]

$$\beta\omega(z) \underset{z\to\infty}{\sim} -\int_{-\infty}^{\infty} \underline{H}^T(z')\underline{C}(z-z')\, dz'\ . \tag{2.43}$$

This is the formally exact asymptote, since the bridge function does not contribute directly because it decays as fast as the short-range part of the direct correlation function. The one-dimensional Fourier transform may be taken in the upper half of the complex plane, and using the same arguments as above one obtains

$$\beta\overline{\omega}(k) \underset{k\to i\kappa}{\sim} -\overline{\underline{H}}^T(k)\left[\frac{4\pi\beta\sigma}{\epsilon\kappa^2}\underline{q} + \overline{\underline{\chi}}(k)\right]\ . \tag{2.44}$$

The wall-ion total correlation function contains a factor of $\underline{\tilde{q}}^T$, which multiplies the bracketed term to give $2\tilde{\sigma}$. Consequently

$$\omega(z) \underset{z\to\infty}{\sim} 2\,\mathrm{Re}\left\{\frac{8\pi\beta\tilde{\sigma}^2}{\epsilon\nu\kappa}e^{-\kappa z}\right\}\ . \tag{2.45}$$

This depends only on properties of the bulk electrolyte, κ and ν, and the effective surface charge of the isolated double layer $\tilde{\sigma}$. Drop the factor of 2 if κ is real. This result shows that the interaction between two double layers is either monotonically repulsive or oscillatory. That is, any attractions measured or predicted cannot persist for all separations, although they can have a very large period of oscillation near the bulk transition. This result also reduces to the linear Poisson-Boltzmann theory in the Debye-Hückel limit $\chi_{\alpha\gamma} = 0$.

2. Core domination

In the core dominated regime, the analysis proceeds as in the bulk. Under the same assumption that the electrolyte ions have identical short-range interactions, one obtains for the spherical solute

$$\underline{\hat{H}}(k;R) \underset{k\to i\xi}{\sim} \frac{-2i\xi x(i\xi)}{\underline{u}^T\underline{u}\,x'(i\xi)(k^2+\xi^2)}\underline{u}\,\underline{u}^T\underline{\hat{\chi}}(i\xi;R)\ . \quad (2.46)$$

The asymptote is

$$h_\alpha(r;R) \underset{r\to\infty}{\sim} 2\,\mathrm{Re}\left\{\frac{-2i\xi}{4\pi n^2 x'(i\xi)}\frac{e^{-\xi r}}{r}\sum_{\gamma>0}\rho_\gamma\hat{\chi}_\gamma(i\xi;R)\right\}\ . \quad (2.47)$$

Since the right hand side is independent of the index of the left hand side, whatever the direct solute-ion interaction for each species is, the solute-ion profiles become identical at large separations in this core-dominated regime (provided that the correlations of the ions themselves are asymptotically identical in the bulk). The solute-solute total correlation function goes like

$$\begin{aligned}\hat{h}_{00}(k;R) &= \hat{c}_{00}(k;R)+\underline{\hat{H}}^T(k;R)\underline{\hat{C}}(k;R)\\ &\underset{k\to i\xi}{\sim}\frac{-2i\xi x(i\xi)}{\underline{u}^T\underline{u}\,x'(i\xi)(k^2+\xi^2)}\\ &\quad\times\underline{\hat{\chi}}^T(i\xi;R)\underline{u}\,\underline{u}^T\underline{\hat{\chi}}(i\xi;R),\end{aligned} \quad (2.48)$$

since the solute-solute direct correlation function is more short ranged than total correlation function and since $\underline{u}^T\underline{\hat{C}} = \underline{u}^T\underline{\hat{\chi}}$ because $\underline{u}^T\underline{q} = 0$. One obtains the asymptote

$$h_{00}(r;R) \underset{r\to\infty}{\sim} 2\,\mathrm{Re}\left\{\frac{-2i\xi}{4\pi n^2 x'(i\xi)}\frac{e^{-\xi r}}{r}\times\left(\sum_{\gamma>0}\rho_\gamma\hat{\chi}_\gamma(i\xi;R)\right)^2\right\}\ . \quad (2.49)$$

Since electrostatics do not enter in the core-dominated regime, one can immediately take the planar limit of this result to obtain the asymptotic ion density profiles off a charged wall,

$$h_\alpha(z) \underset{z\to\infty}{\sim} 2\,\mathrm{Re}\left\{\frac{-2ie^{-\xi z}}{n^2x'(i\xi)}\sum_{\gamma>0}\rho_\gamma\overline{\chi}_\gamma(i\xi)\right\},\quad \alpha>0. \quad (2.50)$$

Finally, it follows from the wall-wall Ornstein-Zernike equation that the interaction free energy per unit area in the core-dominated bulk regime is

$$\beta\omega(z) \underset{z\to\infty}{\sim} 2\,\mathrm{Re}\left\{\frac{-2ie^{-\xi z}}{n^2x'(i\xi)}\left(\sum_{\gamma>0}\rho_\gamma\overline{\chi}_\gamma(i\xi)\right)^2\right\}\ . \quad (2.51)$$

The results obtained in this section (the formal analysis of the asymptotic behavior of the correlation functions) most closely resemble those of Kjellander and Mitchell [13]. The expressions obtained for the effective charge, the screening length and the effective dielectric constant are essentially identical, although perhaps a closer connection is made with the direct correlation function in the present formalism. In addition to the different analysis, here there is an explicit treatment of the oscillatory regime and of the planar limit. Other formal analyses of the screening length [4,5] were exact to order k^2 in the total correlation function, which allowed the screening length to be identified with the isothermal compressibility. (A consequence of the second order approximation is that one only ever obtains either monotonic decay or undamped pure oscillatory decay.) Stell and Lebowitz [6] give the effective charges and the screening length in terms of a compressibility of a reference fluid. These approximate approaches presumably give the first correction to the Debye length at low concentrations, as the pole moves away from the origin, in contrast to the formally exact results that were obtained here and by Kjellander and Mitchell [13].

III. BINARY SYMMETRIC ELECTROLYTE

This section contains results for a restricted primitive model electrolyte that consists of two species identical except for equal and opposite charges. That is, the ions have charge $q_+ = -q_- = q$, hard-sphere diameters $d_+ = d_- = d$, and number density $\rho_+ = \rho_- = n/2$. The pair potential is

$$u_{+,\pm}(r) = u_{-,\mp}(r) = \begin{cases}\infty, & r<d\\ \dfrac{\pm q^2}{\epsilon r}, & r>d,\end{cases} \quad (3.1)$$

where again $\epsilon = 4\pi\epsilon_0\epsilon_r$ is the total permittivity of the medium.

A. Asymptotic analysis

From the symmetry of the pair potential, the correlation matrices contain only two independent components $h_{++}(r) = h_{--}(r)$ and $h_{+-}(r) = h_{-+}(r)$, and similarly for $\underline{\underline{C}}(r)$. The two types of poles discussed in Sec. IV can be analyzed simultaneously by defining $\underline{v}_\pm^T = (1,\pm1)$. Accordingly,

$$\underline{\underline{H}}(r) = h_+(r)\underline{v}_+\underline{v}_+^T + h_-(r)\underline{v}_-\underline{v}_-^T \quad (3.2a)$$

and

$$\underline{\underline{C}}(r) = c_+(r)\underline{v}_+\underline{v}_+^T + c_-(r)\underline{v}_-\underline{v}_-^T, \quad (3.2b)$$

where

$$h_\pm(r) = \frac{n}{4}[h_{++}(r)\pm h_{+-}(r)] \quad (3.3a)$$

and

$$c_\pm(r) = \frac{n}{4}[c_{++}(r)\pm c_{+-}(r)]. \quad (3.3b)$$

Using the orthogonality and potency properties of the dyadics, the Ornstein-Zernike equation becomes

$$\begin{aligned}\underline{\underline{\hat{H}}}(k) &= [\underline{\underline{I}} - \underline{\underline{\hat{C}}}(k)]^{-1}\underline{\underline{\hat{C}}}(k) \\ &= \left[\underline{\underline{I}} - \hat{c}_+(k)\underline{v}_+\underline{v}_+^T - \hat{c}_-(k)\underline{v}_-\underline{v}_-^T\right]^{-1} \\ &\quad \times \left[\hat{c}_+(k)\underline{v}_+\underline{v}_+^T + \hat{c}_-(k)\underline{v}_-\underline{v}_-^T\right] \\ &= \left(\underline{\underline{I}} + \frac{\hat{c}_+(k)}{1-2\hat{c}_+(k)}\underline{v}_+\underline{v}_+^T + \frac{\hat{c}_-(k)}{1-2\hat{c}_-(k)}\underline{v}_-\underline{v}_-^T\right) \\ &\quad \times \left[\hat{c}_+(k)\underline{v}_+\underline{v}_+^T + \hat{c}_-(k)\underline{v}_-\underline{v}_-^T\right] \\ &= \frac{\hat{c}_+(k)}{1-2\hat{c}_+(k)}\underline{v}_+\underline{v}_+^T + \frac{\hat{c}_-(k)}{1-2\hat{c}_-(k)}\underline{v}_-\underline{v}_-^T. \end{aligned} \tag{3.4}$$

If the poles of these two terms occur at $k = i\xi_\pm$, then it follows that

$$\underline{\underline{H}}(r) \underset{r\to\infty}{\sim} 2\,\mathrm{Re}\left\{\frac{-2i\xi_+}{8\pi\hat{c}'_+(i\xi_+)}\frac{e^{-\xi_+ r}}{r}\underline{v}_+\underline{v}_+^T\right\} + 2\,\mathrm{Re}\left\{\frac{-2i\xi_-}{8\pi\hat{c}'_-(i\xi_-)}\frac{e^{-\xi_- r}}{r}\underline{v}_-\underline{v}_-^T\right\}. \tag{3.5}$$

Although both terms exist, only one contributes in the asymptotic limit, depending upon the relative magnitude of $\mathrm{Re}\{\xi_\pm\}$.

1. Electrostatic domination

When $\mathrm{Re}\{\xi_-\} < \mathrm{Re}\{\xi_+\}$, it is the Coulomb part of the pair potential that determines the asymptotic behavior. One has

$$c_-(r) = \frac{n}{4}\left[\chi_{++}(r) - \chi_{+-}(r) - \frac{2\beta q^2}{\epsilon r}\right], \tag{3.6}$$

and the appropriate denominator vanishes when

$$\frac{n}{2}\left[\hat{\chi}_{++}(i\xi_-) - \hat{\chi}_{+-}(i\xi_-) + \frac{8\pi\beta q^2}{\epsilon\xi_-^2}\right] = 1. \tag{3.7}$$

This may be rewritten as

$$\xi_- = \kappa_D \Big/ \sqrt{1 - \frac{n}{2}\left[\hat{\chi}_{++}(i\xi_-) - \hat{\chi}_{+-}(i\xi_-)\right]}. \tag{3.8}$$

The Fourier transform of the short-range part of the direct correlation function is

$$\hat{\chi}_{+\pm}(i\xi_-) = \frac{4\pi}{\xi_-}\int_0^\infty \chi_{+\pm}(r)\sinh(\xi_- r)r\,dr. \tag{3.9}$$

These two equations are in a form suitable for numerical solution for ξ_- by a straightforward iteration procedure.

The total correlation function goes like

$$h_{+\pm}(r) \underset{r\to\infty}{\sim} \pm 2\,\mathrm{Re}\left\{\frac{-2i\xi_-}{8\pi\hat{c}'_-(i\xi_-)}\frac{e^{-\xi_- r}}{r}\right\}, \tag{3.10}$$

where

$$\hat{c}'_-(i\xi_-) = \frac{i\kappa_D^2}{\xi_-^3} + \frac{i\pi n}{\xi_-^2}\int_0^\infty [\chi_{++}(r) - \chi_{+-}(r)] \times [\sinh(\xi_- r) - \xi_- r\cosh(\xi_- r)]\,r\,dr. \tag{3.11}$$

It may be verified that these results correspond to those of Sec. II applied to the binary symmetric electrolyte.

2. Core domination

When $\mathrm{Re}\{\xi_+\} < \mathrm{Re}\{\xi_-\}$, it is the short-range part of the pair potential that determines the asymptotic behavior. One has

$$c_+(r) = \frac{n}{4}\left[\chi_{++}(r) + \chi_{+-}(r)\right], \tag{3.12}$$

and the appropriate denominator vanishes when

$$2\hat{c}_+(i\xi_+) = 1. \tag{3.13}$$

The most straightforward numerical solution of this equation for ξ_+ follows by rearranging the first order Taylor expansion (Newton's method)

$$i\xi_+ = i\xi_+ + \frac{1 - 2\hat{c}_+(i\xi_+)}{2\hat{c}'_+(i\xi_+)}. \tag{3.14}$$

Here

$$\hat{c}_+(i\xi_+) = \frac{\pi n}{\xi_+}\int_0^\infty [\chi_{++}(r) + \chi_{+-}(r)]\sinh(\xi_+ r)r\,dr \tag{3.15}$$

and

$$\hat{c}'_+(i\xi_+) = \frac{i\pi n}{\xi_+^2}\int_0^\infty [\chi_{++}(r) + \chi_{+-}(r)] \times [\sinh(\xi_+ r) - \xi_+ r\cosh(\xi_+ r)]\,r\,dr. \tag{3.16}$$

The total correlation function goes like

$$h_{+\pm}(r) \underset{r\to\infty}{\sim} 2\,\mathrm{Re}\left\{\frac{-2i\xi_+}{8\pi\hat{c}'_+(i\xi_+)}\frac{e^{-\xi_+ r}}{r}\right\}. \tag{3.17}$$

In contrast to the electrostatic-dominated asymptote, the counterion and coion correlations are precisely in phase when the short-range interactions dominate the asymptote. It may be verified that these results correspond to those of Sec. II applied to the binary symmetric electrolyte.

B. Hypernetted chain algorithm

The Ornstein-Zernike equation for the binary symmetric electrolyte was solved together with the hypernetted chain closure (HNC). The usual method of fast Fourier transformation was used. The Coulomb potential was removed from the direct correlation functions at large r, using a function that was well behaved at small r, before they were numerically transformed, and then the

analytic transform of this function was added in Fourier space [21]. Care was taken to transform continuous functions only, and the discontinuity in the direct correlation function and in its first derivative were treated analytically [22]. In summary, only short-ranged, continuous, and well-behaved functions were ever numerically transformed, and consequently it was possible to follow the asymptotic behavior of the pair correlation functions out to many decay lengths.

The HNC is an approximation that is known to be accurate for bulk Coulomb fluids at not too high coupling. Some calculations were performed in the problematic regime using the first resummed bridge diagram [23]. The multidimensional quadrature was carried out by expansion in Legendre polynomials [24], using an orthgonal technique [25]. In most cases HNC total correlation functions were used in the bridge function quadrature. On some occasions, the closure and the quadrature were cycled to self-consistency. For almost all cases examined, the bridge function gave negligible improvement to the HNC, and only results for the bare HNC closure are presented in detail below.

For the Fourier transform, 2^{14} grid points were used, at a spacing of 0.005 Å. Increasing this to 0.02 Å improved results in monovalent electrolytes at the lowest concentrations examined. For the bridge function quadrature, 30 Legendre polynomials were used, and 200 grid points in the radial direction at a spacing of 0.4 Å. Iterations were carried out to six figure convergence in the contact value of the radial distribution funtions. After convergence, the asymptotic parameters were determined, using the trapezoidal rule for the integrals for $\hat{\chi}_{+\pm}(i\xi_{\pm})$ and the two iteration procedures for $\xi_{\pm}$ as described above. Mixing of successive iterates was used and both poles were found. The electrostatic pole was found to be very robust, but the equations for the core pole appeared to possess two or so solutions, and the particular one found could depend upon the starting guess if this pole was the subdominant one. The values given below correspond to the solution with the smallest real part.

C. Numerical results

Figure 1 shows HNC ionic correlation functions in the three different regimes for a monovalent electrolyte. The probabality of finding a counter-ion near a given ion is greater than that of finding a co-ion. This is true everywhere for monotonic correlations, where the two are approximately equal in magnitude but opposite in sign, and is true close to contact in the oscillatory regimes. The distinction between electrostatic domination and core domination is evident in Fig. 1(a) by the relative phase of the two correlation functions. In the electrostatic regime they are out of phase which causes charge density oscillations (here the co-ion total correlation function becomes larger than the counter-ion correlation function at around 10 Å). In the core-dominated regime the correlation functions oscillate in phase which is equivalent to oscillations in number density.

The logarithmic plot [Fig. 1(b)] shows the asymptotic behavior quite clearly. The two oscillatory regimes have

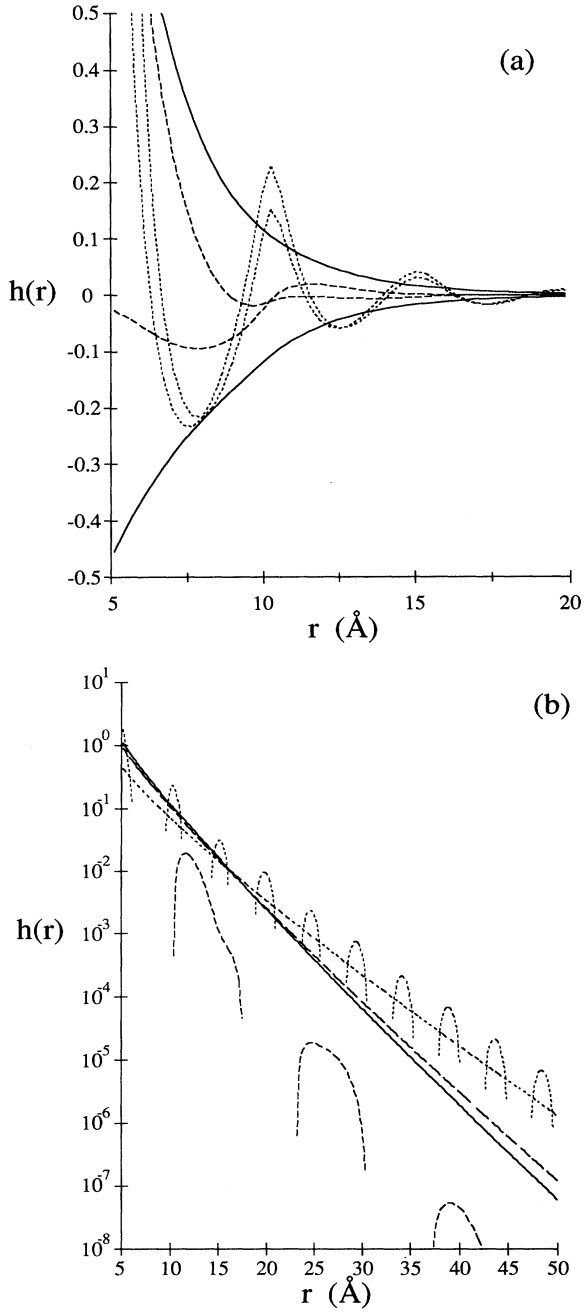

FIG. 1. The total correlation function for a binary symmetric monovalent electrolyte with $d = 5$ Å. Here and in the remaining figures the temperature was 300 K and the relative permittivity was 78.5. (a) HNC results in the monotonic electrostatic regime ($0.5M$, solid curves), in the oscillatory electrostatic regime ($2M$, dashed curves), and in the oscillatory core regime ($5M$, dotted curves). The counter-ion curve is greater than the corresponding co-ion curve near contact. (b) A logarithmic plot of the positive parts of the HNC co-ion total correlation function, with the solid, dashed, and dotted curves corresponding to the monotonic ($0.5M$), electrostatic ($2M$), and core ($5M$) cases, respectively. Also shown for the monotonic case is the modified linearized Debye-Hückel approximation, Eq. (1.29) (dotted line) and the self-consistent analytic approximation, Eqs. (1.39) and (1.41) (dashed line).

markedly different periods of oscillations. In the core-dominated regime, the period is closed to the size of the ions (in this case $d = 5$ Å and the period is 4.8 Å), whereas in the electrostatic regime the period is unrelated to the size of the ions (in this case it is 13.5 Å). In general, the period of oscillations of the pair correlation functions in the electrostatic regime can be expected to be greater than twice the ionic diameter. This is because the two correlations functions oscillate out of phase and correspond to alternate shells of positive and negative charge density about each ion. [Note that only the positive part of the co-ion total correlation functions are shown in Fig. 1(b); the positive parts of the counterion correlation functions would intercalate these in the electrostatic regime and would be superimposed on them in the core regime.]

Also shown in Fig. 1(b) is the co-ion total correlation function in the monotonic regime, as given by the HNC and by two approximate theories. It can be seen that Debye length, which is here equal to 4.3 Å, is not the actual decay length of the electrolyte, which according to the HNC is 3.1 Å. The self-consistent approximation, Eq. (1.39), gives $\kappa^{-1} = 3.3$ Å, and also appears relatively accurate for the magnitude of the pre-exponential factor. It is the size of the error in the decay length that determines the regime of validity of any approximation, since all approximations will eventually be wrong by orders of magnitude at large enough separations because of the exponential decay of the pair correlation functions.

1. *Monotonic regime*

Figure 2 shows the actual decay length of the electrolyte, as given by the hypernetted chain theory and compares the various approximations. All the results converge to the Debye length at low concentrations. For the monovalent electrolytes, with core diameters of 5 and 4 Å, the Debye length is already too large by 10% at around $0.2M$. In the divalent case, the actual decay length is larger than the Debye length at quite small concentrations (e.g., at $0.01M$, it is 17 Å, compared to a Debye length of 15 Å). As the concentration of the divalent electrolyte is increased, the decay length ultimately becomes greater than the Debye length, as was the case for the monovalent electrolyte, which means that in the intermediate regime up to $0.3M$ the Debye length is accurate to within 10%, by happy accident.

The self-consistent analytic approximations for the decay length, Eqs. (1.34), (1.37), and (1.39), describe the decay length of the monovalent electrolytes quite accurately over a substantial part of the monotonic regime. The third order result, Eq. (1.39), is as good as solving the cubic exactly, Eq. (1.37), and is within 10% of the decay length up to $0.9M$ (for d=4 Å, electrostatic oscillations set in beyond $0.95M$, $\kappa_D d = 1.3$). The fact that the two monovalent electrolytes lie on the same curve shows that $\kappa_D d$ is the appropriate dimensionless parameter that characterizes the electrolytes in this regime, as is predicted by the self-consistent approximations.

The decay length in the divalent case clearly lies on a different curve to the monovalents. It is not well described by the self-consistent analytic approximation. However, the nonlinear version, Eq. (1.42), which is also self-consistent with the two moment conditions but which must be solved numerically, is qualitatively correct in predicting that the divalent decay length is first larger than the Debye length, and then smaller, and it may be described as quantitatively accurate at low concentrations. (Note that in this case the monotonic electrostatic regime ends at $0.4M$, $\kappa_D d = 1.6$.) One can conclude that a substantial part of the error in the analytic approximation in the divalent case comes from its linearity; at low concentrations the potential of mean force can be quite large at contact. In the monovalent cases, the nonlinear version is equal to the analytic self-consistent approximations over the whole regime shown, which indicates that the linearization is legitimate here. It is worth mentioning that the HNC results for the decay length may be regarded as exact. Inclusion of the first bridge diagram decreased the decay length of the monovalent electrolyte by 1% at the highest concentration shown.

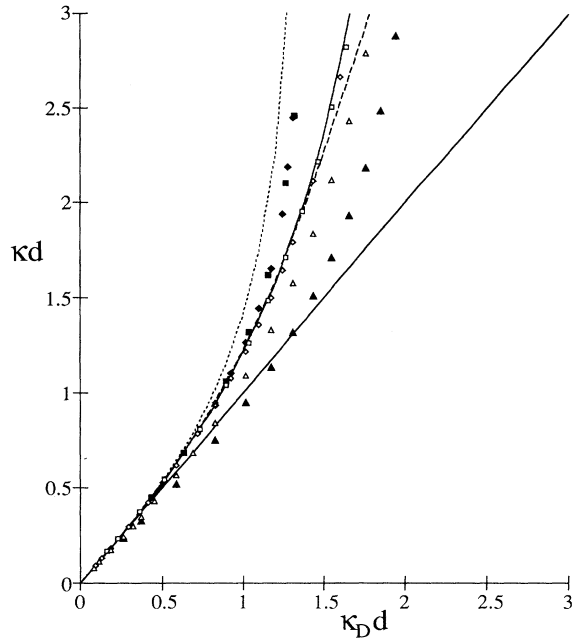

FIG. 2. The decay length of the pair correlation functions as a function of the Debye length, in units of the hard-sphere diameter, in the monotonic regime. The large solid symbols represent HNC calculations; the squares and diamonds are for monovalent ions with $d = 5$ Å and $d = 4$ Å, respectively, and the triangles are for divalent ions with $d = 4$ Å. The straight line is the Debye length, the full curve represents the solution to the cubic equation (1.34), and the dotted and the dashed curves are the analytic expansions (1.37) and (1.39), respectively. The open symbols are the exponential approximation (1.42).

Figure 3 shows the excess internal energy per ion. For the present binary symmetric electrolyte this is

$$\beta u^{\mathrm{ex}} = \pi n \Gamma d \int_d^\infty [h_{++}(r) - h_{+-}(r)] r \, dr, \qquad (3.18)$$

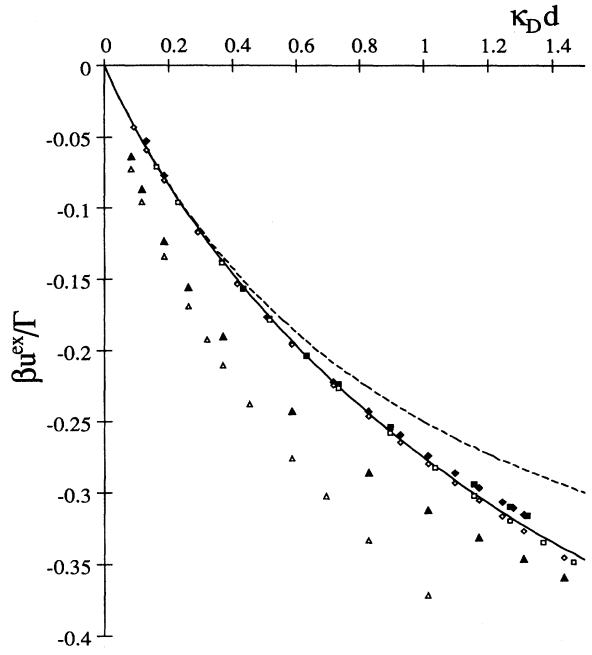

FIG. 3. The excess internal energy per ion, normalized by the coupling constant $\Gamma = \beta q^2/\epsilon d$. The symbols are as before, the solid curve uses the approximation (1.39), and the dashed curve uses the Debye-Hückel approximation (1.29).

where the dimensionless coupling constant is $\Gamma = \beta q^2/\epsilon d$. This integral was evaluated numerically for the HNC and for the nonlinear approximation. In the linear cases one obtains

$$\beta u^{\mathrm{ex}} = \frac{-\Gamma\kappa d}{2(1+\kappa d)}, \tag{3.19}$$

with κ being equal to κ_D for the modified Debye-Hückel approximation, Eq. (1.29), and being given by Eq. (1.39) in the self-consistent case. It can be seen in the figure that the results for the monovalent electrolyte are given quite accurately by the self-consistent approximations, and that the Debye-Hückel theory significantly underestimates the magnitude of the internal energy. The nonlinear self-consistent theory gives the energy accurately in the divalent electrolyte at low concentrations, but overestimates the correction to the linear theory as the concentration is increased. Including the first bridge diagram in the HNC increased the magnitude of the internal energy by about 0.2% at $5M$ concentration of the divalent electrolyte ($\kappa_D d = 6.8$), and by even smaller amounts for the monovalent electrolytes. Hence the HNC may be taken as an accurate benchmark to test the more approximate theories, as has been done here.

In general, the pressure is more sensitive to approximations than the energy. The osmotic coefficient is given by

$$\phi = \frac{p_v}{nk_BT} = 1 + \frac{\beta u^{\mathrm{ex}}}{3} + \frac{\pi n d^3}{3}[2 + h_{++}(d^+) + h_{+-}(d^+)]. \tag{3.20}$$

For the linear theories, the nontrivial parts of the bracketed term cancel. The osmotic coefficient is plotted in Fig. 4, and it can be seen that only the nonlinear self-consistent theory is quantitatively accurate. This is probably due to the significant contribution from the contact value of the correlation functions, which cancels identically in the linear theories. The nonlinear self-consistent theory exaggerates the turn up in the HNC data as the concentration is increased. In the case of the $5M$ divalent electrolyte, inclusion of the first bridge diagram decreases the osmotic coefficient by about 3%.

2. *Oscillatory regime*

Figures 5 show the characteristic lengths of the correlation function, mainly in the oscillatory regime. The total correlation function may be written

$$h_{++}(r) = A\cos[\kappa_i(r-\delta)]e^{-\kappa_r r}/r. \tag{3.21}$$

The decay length is κ_r^{-1}, and the period of the oscillations is $2\pi/\kappa_i$. Oscillations are signified by nonzero values of κ_i. The amplitude is A and the phase is δ. The lengths corresponding to both poles, the electrostatic and the core, are plotted; the pole which dominates the asymptotic behavior is the one with the larger decay length.

In Fig. 5(a) (monovalent electrolyte, d=5 Å), electrostatic oscillations begin at $0.65M$ ($\kappa_D d = 1.3$), which is somewhat less than the Stillinger-Lovett [2] upper bound

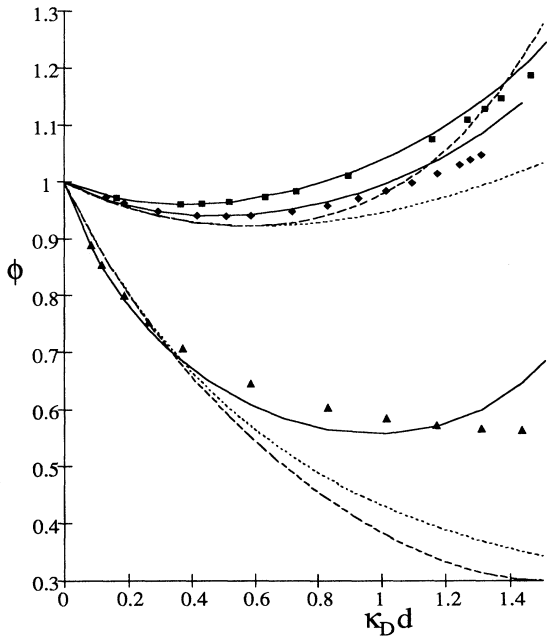

FIG. 4. The osmotic coefficient. The symbols are the HNC (as above), the solid curve uses the exponential approximation (1.42), the dashed curve uses the analytic moment approximation (1.39), and the dotted curve uses the Debye-Hückel approximation (1.29). The latter two aproximations are shown for the monovalent and divalent electrolytes with d = 4 Å only.

$\sqrt{6} = 2.4$, but which is rather close to the pole of the Padé approximant, Eq. (1.37), $\sqrt{2} = 1.4$. At the onset of the oscillations the period diverges, which makes sense since the monotonic regime may simply be regarded as having an infinite period of oscillation. The smallest period observed for the electrostatic oscillations was about 8 Å (at a concentration of $8M$). This is slightly less than twice the ionic diameter, which is consistent with the picture discussed above of alternating shells of charge. At the transition from monotonic to oscillatory behavior, the decay length changes from a decreasing function of concentration to a slowly increasing one. It can be seen that the decay length due to the core pole is increasing more quickly and first exceeds the electrostatic decay

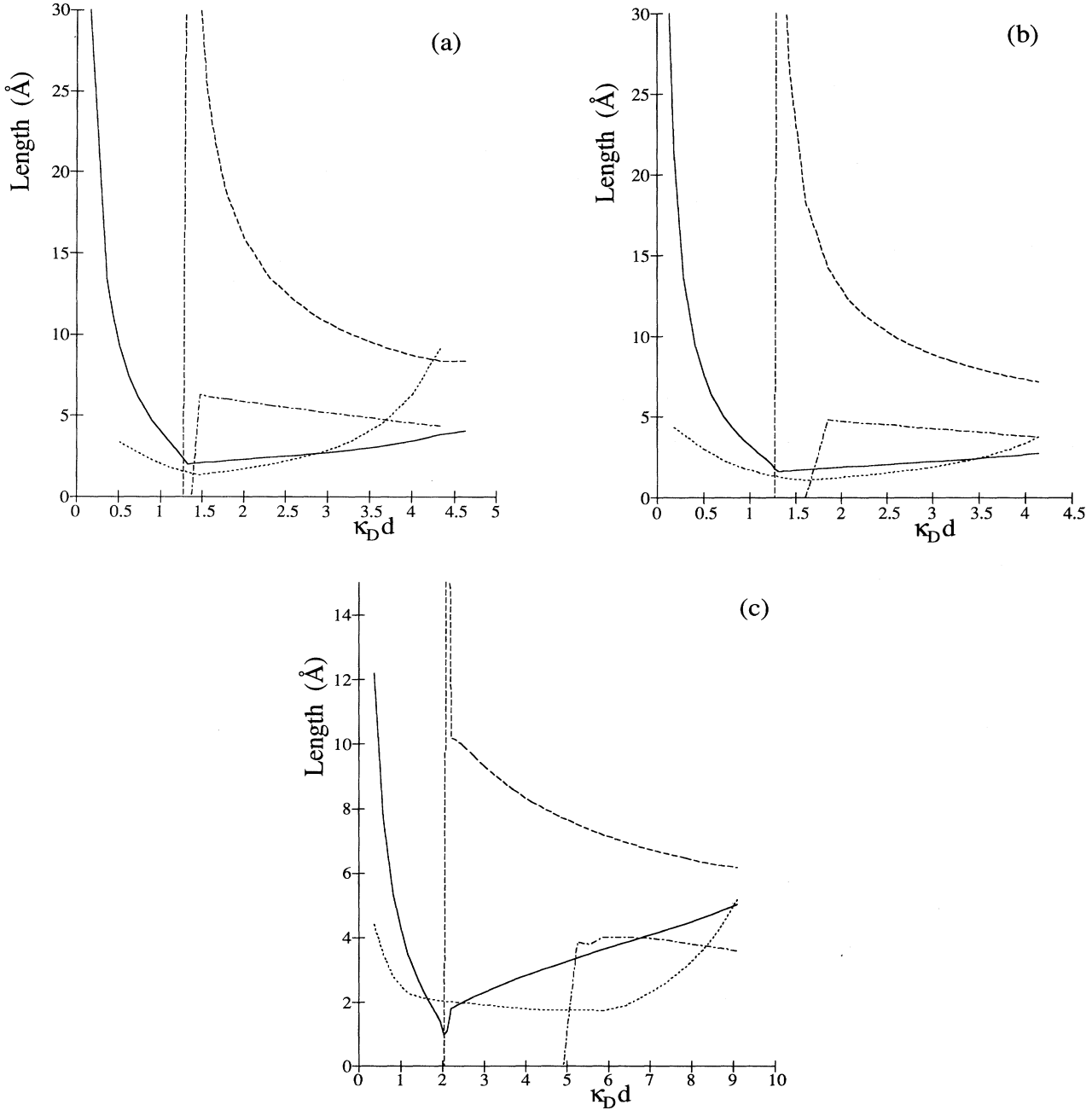

FIG. 5. The decay length κ_r^{-1} and the period of the oscillations $2\pi/\kappa_i$ for the electrolytes as a function of $\kappa_D d$. The full curve is κ_r^{-1} and the dashed curve is $2\pi/\kappa_i$ for the electrostatic pole, and these quantities for the core pole are respectively given by the dotted curve and the dash-dotted curve. Note that the behavior in the asymptotic regime is determined by the pole with the larger decay length. (a) Monovalent electrolyte, $d = 5$ Å. (b) Monovalent electrolyte, $d = 4$ Å. (c) Divalent electrolyte, $d = 4$ Å.

length at $\kappa_D d = 3.0$ ($3.5M$). The period is close to 5 Å, the ionic diameter, and is a decreasing function of concentration. Although the ionic diameter represents the distance of closest approach of two ions, a little thought suggests that in a dense fluid the pair correlation function should oscillate somewhat more frequently than this, due to many-body packing effects on the spherical average. At $7M$, the period was $0.87d = 4.4$ Å.

Figure 5(b) shows the relevant lengths in monovalent electrolyte with $d = 4$ Å. The behavior is qualitatively similar to the 5 Å case, with monotonic decay at low concentrations, electrostatic oscillations in the intermediate regime, and core oscillations in the dense electrolyte. In this case the monotonic-oscillatory transition occurs at $\kappa_D d = 1.3$, or $0.95M$, and the electrostatic-core transition is at $\kappa_D d = 3.6$, or $7.5M$. The first transition is at about the same value of the parameter $\kappa_D d$ as for the $d = 5$ Å case, but the second transition occurs at a value approximately 20% larger. Over much of the oscillatory regime shown, the decay lengths due to the two poles are almost equal, which indicates that both will make a non-negligible contribution to the total correlation function over substantial separations of the ions, even though only one will eventually dominate asymptotically. This is one reason why the asymptotic behavior is more easily determined using the present analysis than by attempting to fit the correlation functions themselves.

The behavior of the divalent electrolyte is more complicated than the monovalents. In Fig. 5(c), the electostatic decay length initially decreases with concentration in the monotonic regime, and then at $0.6M$ ($\kappa_D d = 2.0$) electrostatic oscillations set in and the decay length begins to increase with concentration. (The significance of the structure around the transition is unclear.) However, between $0.4M$ and $0.9M$ ($\kappa_D d = 1.7 - 2.5$), the core pole has the larger decay length. In this regime the counter-ion and co-ion total correlation functions are equal in sign and decay monotonically to zero. The core pole does not yield oscillatory behavior until $3.5M$ ($\kappa_D d = 4.9$). By this time the electrostatic pole is once more the dominant one, and the period of the electrostatic oscillations is 10–6 Å. It is not until $11M$ ($\kappa_D d = 8.9$) that the core finally wins out, and here the period of the core oscillations is 3.6 Å.

Figure 6 shows the amplitude of the asymptote of the total correlation function. In Fig. 6(a), the electrostatic amplitude is shown. The Debye-Hückel result, $|A| = \beta q^2/\epsilon$, which is independent of concentration, is indeed the correct limiting result for vanishing concentrations, but rapidly becomes invalid at finite concentrations. The HNC amplitude approaches this limit from above in the monovalent electrolytes and from below in the divalent. At the monotonic-oscillatory transition, the divergence in the amplitude discussed above, Eq. (2.16), is clear. The hiccup in the divalent curve just prior to transition may not be significant; in this regime the core pole dominates the asymptote. Figure 6(b) shows the amplitude of the core pole. The peak again corresponds to the oscillatory-monotonic transition. In the oscillatory regime, the monovalent curves are coincident, which indicates that the amplitude is here only a function of $\kappa_D d$. This is not so for the divalent electrolyte. In this case, the oscillatory-monotonic transition is broader and is not characterized by a single sharp peak.

Figure 7 shows the phase of the oscillatory asymptote in the monovalent electrolyte. In these units the phases

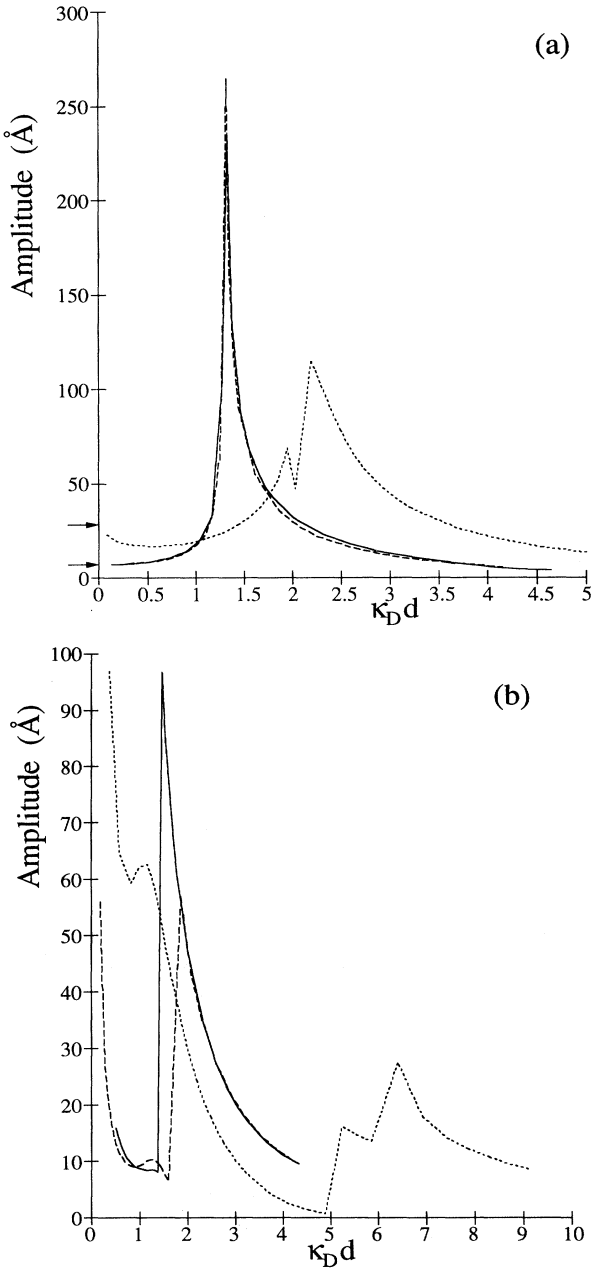

FIG. 6. The amplitude of the asymptote for the pair correlation functions as a function of concentration. The full curve is for monovalent electrolyte, $d = 5$ Å, the dashed curve is for monovalent electrolyte, $d = 4$ Å, and the dotted curve is for divalent electrolyte, $d = 4$ Å. (a) The electrostatic asymptote; the arrows denote the limiting values given by the linearized Debye-Hückel approximation, Eq. (1.28). (b) The core asymptote.

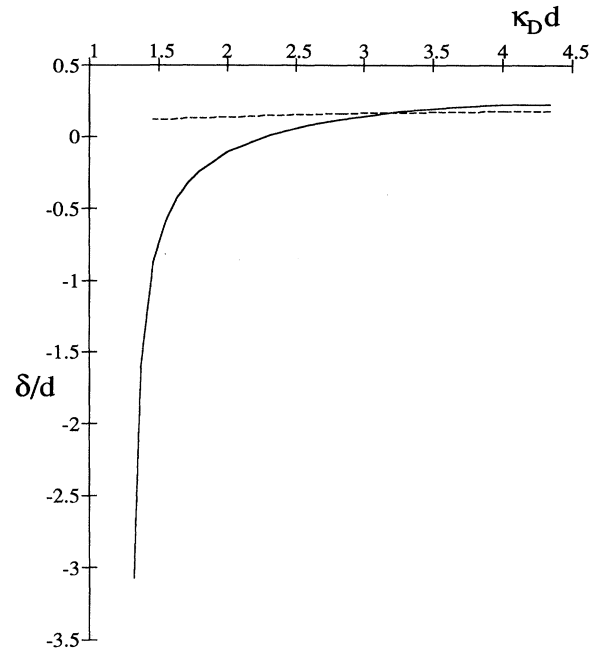

FIG. 7. The phase of the oscillations of the asymptote in the monovalent electrolyte, in units of the hard-sphere diameter. The full curve is for the electrostatic asymptote and the dashed curve is for the core asymptote.

of the 4 and 5 Å diameter ions are identical. For the case of the core pole, where the period of oscillations is close to the diameter of the ions, the peaks in the correlation function are shifted out from contact by about one-quarter diameter. The phase in the divalent electrolyte (not shown) is qualitatively similar, but exhibits some steps just after the oscillatory transition, reflecting the behavior of the amplitude in this regime.

With all asymptotic expansions there remains the question of the regime of validity. This is explored in Fig. 8 for the monovalent electrolyte with $d = 5$ Å. In Fig. 8(a), which at $2M$ is in the electrostatic dominant regime, the HNC electrostatic asymptote may be seen to be applicable beyond about 13 Å. The departure of the HNC data from exact asymmetry $[h_{++}(r) = -h_{+-}(r)]$ is due to the contribution of the core in the nonasymptotic regime. Hence the figure also includes curves that consist of setting the potential of mean force equal to the sum of the electrostatic and the core asymptotes. It can be seen that this nonlinear approximation, which beyond about 15 Å equals the electrostatic asymptote, is already valid at about 8 Å. Similar conclusions may be made of the data in Fig. 8(b) ($5M$, core dominant). Apart from overestimating the depth of the first minimum, the core asymptote alone is virtually quantitively accurate for all separations. The small asymmetry is nearly entirely accounted for by adding the electrostatic asymptote to the potential of mean force. It is pleasantly surprising that the eight asymptotic parameters are sufficient to describe the HNC data over almost the whole separation regime.

CONCLUSION

This paper has been concerned with the theory of primitive model electrolytes and the electrical double layer. Both approximate and formally exact analyses were made

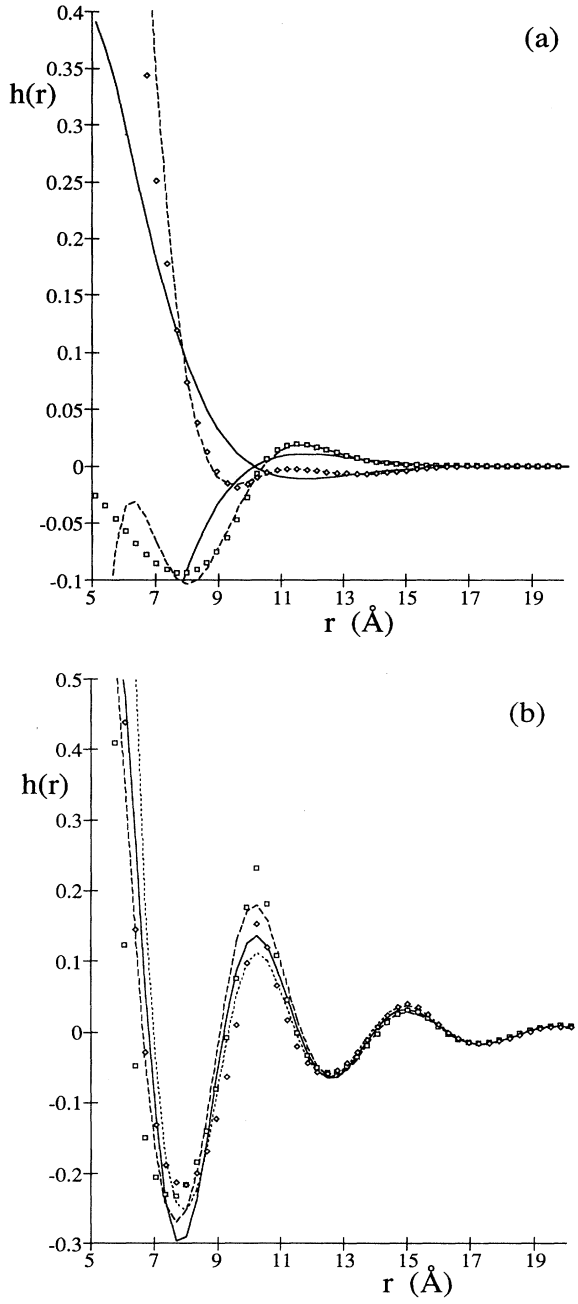

FIG. 8. The total correlation functions for the monovalent electrolyte with $d = 5$ Å. The symbols represent the full HNC function (the squares are for co-ions, and the diamonds are for counter-ions). The solid lines represent the asymptote and the broken lines result from setting the potential of mean force equal to the sum of the core and electrostatic asymptotes. (a) $2M$, electrostatic domination. (b) $5M$, core domination.

of the Ornstein-Zernike equation using the fact that the direct correlation function decays like the Coulomb potential at long range. The main approximate result was an analytic expression for the decay length in the electrolyte, derived by satisfying the exact second moment condition with a Yukawa form for the total correlation function. The result was shown to be fairly accurate by comparison with hypernetted chain calculations, and to greatly enhance the applicability of the classic Debye-Hückel theory. The results of the asymptotic analysis were a formally exact expression for the decay length in terms of effective charges on the ions, and an expression for the latter in terms of integrals of the short-range part of the direct correlation function. The analysis enabled the three asymptotic regimes —monotonic, electrostatic-dominated oscillatory, and core-dominated oscillatory— to be clearly distinguished. The analysis was extended to the spherical and the planar electrical double layers, where it was shown that the decay of the density profile due to an isolated solute or charged wall, and also the decay of the interaction free energy, was the same as for the bulk correlation functions of the electrolyte. The approximate and exact theories were tested by numerical hypernetted chain calculations, and the asymptotic phase diagram of several aqueous electrolytes was explored.

ACKNOWLEDGMENTS

Jonathan Ennis has independently performed a similar numerical hypernetted chain study of the asymptotic phases of a primitive model electrolyte [17], and I thank him for providing some references.

[1] P. Debye and E. Hückel, Z. Phys. **24**, 185 (1923); **24**, 305 (1923).
[2] F.H. Stillinger and R. Lovett, J. Chem. Phys. **48**, 3858 (1968).
[3] F.H. Stillinger and R. Lovett, J. Chem. Phys. **49**, 1991 (1968).
[4] P.V. Giaquinta, M. Parrinello, and M.P. Tosi, Phys. Chem. Liq. **5**, 305 (1976).
[5] P. Vieillefosse, J. Phys. (Paris) Lett. **38**, L43 (1977).
[6] G. Stell and J.L. Lebowitz, J. Chem. Phys. **48**, 3706 (1968).
[7] D.J. Mitchell and B.W. Ninham, Chem. Phys. Lett. **53**, 397 (1978).
[8] M. Parrinello and M.P. Tosi, Riv. Nuovo Cimento **2** (6), 1 (1979).
[9] F.H. Stillinger and R. Lovett, J. Chem. Phys. **48**, 3869 (1968).
[10] C.W. Outhwaite, Stat. Mechan. Specialist Periodical Rep. **2**, 188 (1975).
[11] L. Blum, Mol. Phys. **30**, 1529 (1975).
[12] L. Blum and J.S. Høye, J. Phys. Chem. **81**, 1311 (1977).
[13] R. Kjellander and D. John Mitchell, Chem. Phys. Lett. **200**, 76 (1992).
[14] M.E. Fisher and B. Widom, J. Chem. Phys. **50**, 3756 (1969).
[15] R. Evans, J.R. Henderson, D.C. Hoyle, A.O. Parry, and Z.A. Sabeur, Mol. Phys. (to be published).
[16] G. Stell, K.C. Wu, and B. Larsen, Phys. Rev. Lett. **37**, 1369 (1976).
[17] J.P. Ennis, Ph.D. thesis, Australian National University, 1993 (unpublished).
[18] P. Attard, C.P. Ursenbach, and G.N. Patey, Phys. Rev. A **45**, 7621 (1992).
[19] P. Attard and S. Miklavic, J. Chem. Phys. (to be published).
[20] P. Attard, D.R. Bérard, C.P. Ursenbach, and G.N. Patey, Phys. Rev. A **44**, 8224 (1991).
[21] J.F. Springer, M.A. Pokrant, and F.A. Stevens, J. Chem. Phys. **58**, 4863 (1973).
[22] P. Attard and G.N. Patey, J. Chem. Phys. **92**, 4970 (1990).
[23] H. Iyetomi and S. Ichimaru, Phys. Rev. A **27**, 1241 (1983).
[24] R. Bacquet and P.J. Rossky, J. Chem. Phys. **79**, 1419 (1982).
[25] P. Attard, J. Chem. Phys. **91**, 3072 (1989).